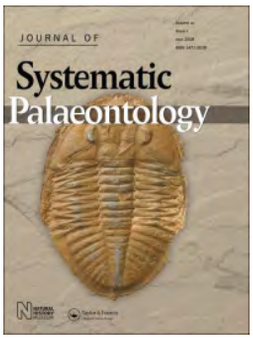

Journal of Systematic Palaeontology

ISSN: (Print) (Online) Journal homepage: www.tandfonline.com/journals/tjsp20

Taxonomic revision of the late Permian dicynodont genus *Endothiodon* (Therapsida, Anomodontia)

Iyra E. M. Maharaj, Zanildo Macungo, Roger M. H. Smith, Anusuya Chinsamy & Ricardo Araújo

To cite this article: Iyra E. M. Maharaj, Zanildo Macungo, Roger M. H. Smith, Anusuya Chinsamy & Ricardo Araújo (2024) Taxonomic revision of the late Permian dicynodont genus *Endothiodon* (Therapsida, Anomodontia), Journal of Systematic Palaeontology, 22:1, 2346578, DOI: 10.1080/14772019.2024.2346578

To link to this article: https://doi.org/10.1080/14772019.2024.2346578

Journal of Systematic Palaeontology, 2024
Vol. 22, No. 1, 2346578
http://dx.doi.org/10.1080/14772019.2024.2346578

Taylor & Francis
Taylor & Francis Group

Taxonomic revision of the late Permian dicynodont genus *Endothiodon* (Therapsida, Anomodontia)

Iyra E. M. Maharaj[a]*, Zanildo Macungo[b,c], Roger M. H. Smith[c,d], Anusuya Chinsamy[a] and Ricardo Araújo[b,e]*

[a]*Department of Biological Sciences, University of Cape Town, Cape Town, South Africa;* [b]*Museu Nacional de Geologia, Maputo, Mozambique;* [c]*Evolutionary Studies Institute, University of the Witwatersrand, Johannesburg, South Africa;* [d]*Karoo Palaeontology, Iziko South African Museum, Cape Town, South Africa;* [e]*Instituto de Plasmas e Fusão Nuclear & Centro de Recursos Naturais e Ambiente (CERENA), Instituto Superior Técnico, Universidade de Lisboa, Lisbon, Portugal*

(Received 19 June 2023; accepted 4 April 2024)

The dicynodont genus *Endothiodon*, known for its unusual anatomy and possession of multiple tooth rows in some specimens, has a complex taxonomic history. We conducted a comprehensive review of 150 *Endothiodon* specimens from South Africa, Mozambique, Tanzania, Malawi, Zambia, Brazil and India to clarify taxonomy, diagnose species and understand relationships. Additionally, we analysed the biostratigraphic distribution of South African *Endothiodon* specimens, confined to the *Endothiodon* Assemblage Zone (AZ). Using 24 specimens, including four outgroup taxa, we created a character matrix with 22 new characters. Phylogenetic analysis revealed three clades: a basal clade representing the species *Endothiodon mahalanobisi* and two clades formed by the species *Endothiodon tolani* and *Endothiodon bathystoma. Endothiodon bathystoma* is diagnosed by a large pineal boss, *E. tolani* by an enlarged caniniform and a thin collar of bone around the pineal foramen, and *E. mahalanobisi* by an unornamented pineal foramen. '*Endothiodon uniseries*' subsumes within *E. bathystoma*, suggesting that tooth row count must be used with caution as a character. *Endothiodon mahalanobisi* is exclusive to India, whereas all three of the valid *Endothiodon* species co-occur in Mozambique, whilst South African specimens exclusively represent *E. bathystoma*. Assuming contemporaneous deposition, a longitudinal gradient of *Endothiodon* diversity is evident, with East African basins harbouring the greatest diversity. This taxonomic revision clarifies the species diversity, intrageneric relationships and geographical distribution of *Endothiodon*. Our findings contribute to understanding the evolutionary history of these unique dicynodonts and emphasize the importance of considering both anatomical characteristics and geographical patterns in taxonomic investigations.

Keywords: *Endothiodon*; Dicynodontia; taxonomy; biostratigraphic distribution; phylogenetic analysis

Introduction

Among dicynodonts, the taxonomy of the late Permian genus *Endothiodon* has been problematic for decades (Cox, 1964; Cox & Angielczyk, 2015; Macungo et al., 2019) despite the abundance of fossils recovered from South Africa (Maharaj et al., 2021; Owen, 1876), Mozambique (Araújo et al., 2018, 2020; Latimer et al., 1995; Macungo et al., 2019), Tanzania, Zambia and Malawi (Angielczyk et al., 2014; Cox & Angielczyk, 2015; Dias-da-Silva, 2012; Fröbisch, 2009; Haughton, 1926; Kitching, 1963; Jacobs et al., 2005), India (Ray, 2000; Ray & Bandyopadhyay, 2003), and Brazil (Boos et al., 2013). The taxonomic complexity of the genus has been aggravated by the persistent addition and removal of new species and genera to and from Endothiodontidae since Owen's (1876) original definition of the family. It may be pertinent to explicitly emphasize that historical conceptions of Endothiodontidae have, at times, been considerably broader than recent interpretations, essentially encompassing all dicynodonts possessing postcanine teeth. Notable publications employing this taxonomic framework include those by Broom (1904a, 1904b, 1904c), Keyser (1993), Toerien (1953) and van Hoepen (1934). As *Endothiodon* research continued into the twentieth century, specimens were often re-assigned based on newly revealed features which consequently increased taxonomic instability (Broili & Schöder, 1936; Broom, 1900, 1904a, 1904b, 1904c, 1904d, 1911, 1912, 1915, 1921, 1923, 1932; Cox, 1964; Cox & Angielczyk, 2015; Lydekker, 1890; Owen, 1876, 1879; Ray, 2000; Seeley, 1892, 1894; see also Figs 1, 2). Until now, *E. bathystoma* was known from South Africa, Mozambique and possibly Tanzania and Zambia (Cox & Angielczyk, 2015), *E. uniseries* from South Africa and India (Cox, 1964; Ray, 2000), *E. tolani* from Tanzania, Zambia and Mozambique (Cox & Angielczyk, 2015; Macungo et al., 2019) and *E. mahalanobisi* from India (Ray, 2000). However, despite significant revisions (Cox, 1964; Cox

*Corresponding authors. Emails: iyraem@gmail.com; ricardo.araujo@tecnico.ulisboa.pt

Published online 30 May 2024

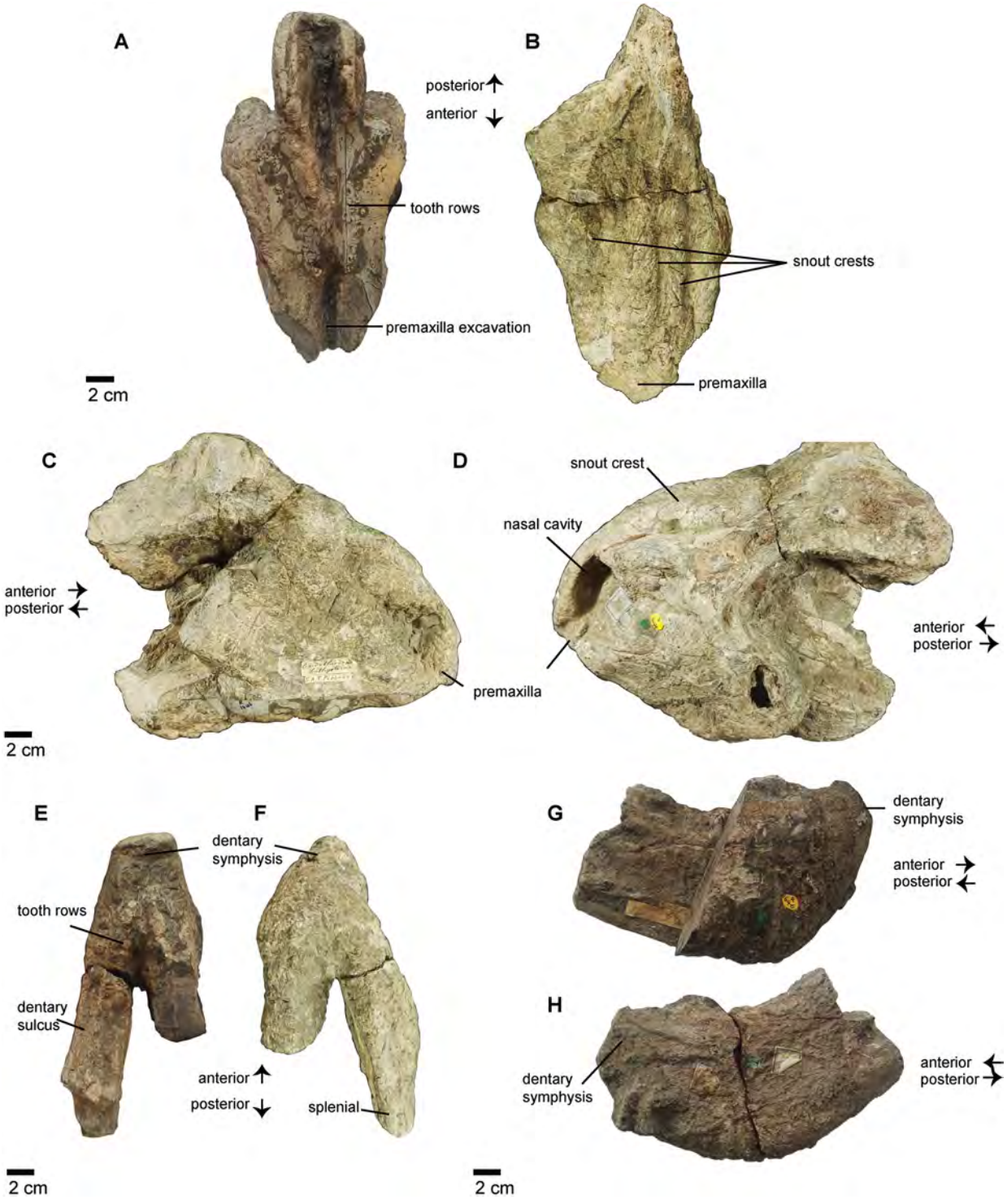

Figure 1. Photographs of the *Endothiodon bathystoma* holotype described by Owen (1876: NHMUK PV R1646). **A**, anterior skull in ventral view showing palate with one tooth row and replacement teeth; **B**, dorsal view. Anterior skull in **C**, right and **D**, left lateral views. **E**, dentary in dorsal view with multiple tooth rows; and **F**, ventral view. Dentary in **G**, left and **H**, right lateral views.

& Angielczyk, 2015) and further *Endothiodon* material being recovered from Mozambique (Macungo et al., 2019), there is still no clear consensus on the validity of all the *Endothiodon* species, the taxonomic relevance of certain anatomical features, the extent of intraspecific variation within *Endothiodon* species, and their

Year	Author	Identification	Features
1876	Owen, R.	*Endothiodon bathystoma* gen. n., sp. nov.	• Small, round scattered teeth • Teeth on palatal surface of maxilla and palatine bones • No teeth on alveolar borders of maxilla and premaxilla
1879	Owen, R.	*E. bathystoma* additional features	• No canine socket/germ tooth • 3 rows of palatal teeth • 3 rows of similarly shaped, smaller lower jaw teeth
		Endothiodon uniseries sp. n.	• Smaller specimen • 1 row of teeth • Caniniform process like a "dental weapon"
1890	Lydekker, R.	*Endothiodon* additional features	• Upper teeth on maxilla bone, not palatine & vomer
		Theriognathus microps → *E. uniseries* (particular specimen)	• Smaller • "Very small" orbits • 1 row palatal teeth
1892	Seeley, H.G.	*E. bathystoma* additional features	• Teeth embedded in jaw sockets • Articular condyle different from other dicynodonts • Large parietal foramen
1894	Seeley, H.G.	*E. uniseries* → *Esoterodon uniseries* gen. n., sp. nov.	
		Cryptocynodon simus → an endothiodont	• No incisor teeth • Hard palate imperfectly developed • No coronoid process on lower jaw
1904	Broom, R.	*Prodicynodon pearstonensis* gen. n., sp. nov.	• Postcanine teeth
		Opisthoctenodon agilis gen. n., sp. nov.	• Postcanine teeth; pointed beak
		Chelyoposaurus williamsi gen. n., sp. nov.	• Postcanine tooth; enormous squamosal
1912	Broom, R.	*Endothiodon whaitsi* sp. n.	• 2X size of *E. uniseries* • Nasals do not overhang nostrils • Small pineal foramen
		Endothiodon platyceps sp. n.	• No teeth serrations • Double row of teeth "behind" • Flat, broad head • Smaller teeth
		E. platyceps → *Emydochampsa platyceps* gen. n., sp. nov. → *Endothiodon platyceps* (addendum in same paper)	
1915	Broom, R.	*Esoterodon uniseries* → *Endothiodon uniseries*	• No valid difference
		Endothiodon seeleyi sp. n. (based on 1 specimen)	• Different teeth to *E. bathystoma*
		Emydochampsa platyceps → *Endothiodon platyceps*	• Teeth not distinct enough
		Endothiodon paucidens sp. n.	• Differs from *E. uniseries* and *E. whaitsi*
1921	Broom, R.	*Endothiodon crassus* sp. n.	• Broad, flat • Skull broader than long • Very broad nasals
1923	Broom, R.	*Endothiodon angusticeps* sp. n.	• Longer, slenderer lower jaw than *E. uniseries*
1932	Broom, R.	*E. uniseries, E. angusticeps, E. whaitsi, E. paucidens* → *Esoterodon*	• Revert to Seeley's assignment to *Esoterodon* • Single row of upper teeth
		Endogomphodon minor gen. n., sp. nov.	• Short, broad snout • 6 teeth on each side, irregular anteriorly
1936	Broili, F. & Schröder, J.	*Emydochampsa oweni* sp. n.	• Anterior lower teeth in single row • Posterior lower teeth irregular
1964	Cox, C.B.	**MAJOR REVISION:** → *ENDOTHIODON* IS THE ONLY VALID GENUS: *E. bathystoma*, *E. whaitsi*, *E. uniseries*	
2000	Ray, S.	*Endothiodon mahalanobisi* sp. n.	• 1 ridge on snout • Elliptical pineal foramen • Slender dentary
2015	Cox, C.B. & Angielczyk, K.D.	*Pachytegos stockleyi* → *E. bathystoma*	• No valid difference
		Endothiodon tolani sp. n.	• Pineal foramen surrounded by thin collar of bone • No pineal boss • Caniniform tusks

stratigraphic congruence. Here, we test the taxonomic validity of the three currently accepted *Endothiodon* species (*E. tolani*, *E. bathystoma*, and *E. mahalanobisi*; Cox & Angielczyk, 2015). The aim of this study, therefore, is to re-assess the taxonomic validity of previously proposed *Endothiodon* species, and to subject previously reported specimens to an informed taxonomic assessment. The present abundance of *Endothiodon* cranial remains provides, for the first time, an opportunity to conduct a taxonomic review of the genus using phylogenetic analyses. Furthermore, recent refinement of the tetrapod biozonation of the South African Karoo Supergroup presents an opportunity to more accurately position South African *Endothiodon* specimens within the stratigraphic intervals from which they were recovered.

The convoluted history of *Endothiodon*

Endothiodon was initially described by Owen (1876), who attributed an anterior skull fragment and associated mandible to the type species, *Endothiodon bathystoma* (Figs 1A–D, 2). Owen (1876) differentiated this species by its unique dentition, characterized by teeth with a circular cross-section. Subsequently, Owen (1879) provided further details on this specimen, along with another mandible resembling *E. bathystoma*, confirming the presence of multiple rows of teeth (Fig. 1A, C). These tooth rows were considered a distinguishing feature and were suggested to be specialized for crushing invertebrates. Upon examining the maxilla of the type specimen, no traces of a tooth socket or enlarged caniniform were found (note: we use the term ‘tuskless’ when an *Endothiodon* does not possess an enlarged caniniform). In the same publication, Owen (1879) introduced *E. uniseries* as a new, smaller species with a single row of teeth in both jaws, contrasting with the multiple tooth rows observed in *E. bathystoma*. Owen (1879, p. 559) likened the ventral premaxillary projection of *E. uniseries* to the "'tooth' as that part in the beak of the Falcon". Based on these distinctions, Owen (1879) proposed that *Endothiodon* deserved its own family classification within Anomodontia. Between Owen's (1876) initial description of *Endothiodon* and Cox's (1964) significant revision of the genus, multiple papers (Broom, 1900, 1904a, 1904b, 1904c, 1904d, 1911, 1912, 1913, 1915, 1921, 1923, 1932; Broili & Schöder, 1936; Lydekker, 1890; Seeley, 1892, 1894) re-evaluated and added diagnostic traits to endothiodonts. Following the introduction of *E. uniseries*, additional taxa were included in the taxonomic concept of the family Endothiodontidae at that time, such as *Diaelurodon whaitsi* (Broom, 1911) now considered a junior synonym of *Pristerodon mackayi*, *E. whaitsi* and *E. platyceps* (Broom, 1912), *E. seeleyi* and *E. paucidens* (Broom, 1915), *E. crassus* (Broom, 1921) and *E. oweni* (Broili & Schöder, 1936). Figure 2 provides an overview of the species and genus assignments to the family since 1876.

Despite Cox's (1964) warning about the challenges of distinguishing species based on size, he grouped smaller specimens under *E. uniseries*. As a result of the revision, the number of species was reduced from nine to three: *E. bathystoma*, *E. whaitsi* and *E. uniseries*. Cox (1964) acknowledged *Pachytegos stockleyi* as a distinct genus and species, but later Cox and Angielczyk (2015) synonymized it with *E. bathystoma*. While emphasizing the importance of re-evaluating published descriptions, Cox (1964) cautioned that even in his revision, these species remained incompletely defined, highlighting the need for further taxonomic research. Since then, *Endothiodon* taxonomy has been addressed in multiple studies, including Ray (2000), Boos et al. (2013), Cox and Angielczyk (2015), and Macungo et al. (2019). Ray (2000) presented the first detailed description of *Endothiodon* from outside Africa, introducing the new species *E. mahalanobisi* discovered in the Kundaram Formation of India, where *E. uniseries* was also found (Bandyopadhyay & Ray, 2020). Boos et al. (2013) re-described a partial skull and dentary of *Endothiodon*, which was the first dicynodont occurrence from the Permian of South America (Barberena & Araújo, 1975; Barberena et al., 1985). The material was incomplete and could not be identified to species level. Cox and Angielczyk (2015) later described material from Tanzania as a new species, *E. tolani*, diagnosed by the presence of a thin collar of bone surrounding the pineal foramen and enlarged caniniforms.

Macungo et al. (2019) presented detailed cranial and postcranial anatomy in their description of *Endothiodon* from the Metangula Graben of Mozambique. The material contained some specimens displaying the *E. bathystoma*-like morphotype (tuskless; developed pineal boss) and others displaying the *E. tolani*-like morphotype (enlarged caniniforms; no pineal boss). The pineal boss was re-assessed for its taxonomic value, but the fact that it is susceptible to becoming separated during the post-mortem-preburial phase of fossilization requires careful assessment of this character. Pineal bosses in the Permian dicynodont *Diictodon* may be sexually

Figure 2. Timeline summarizing the taxonomic history of *Endothiodon*. The red arrows indicate taxonomic revisions, and diagnostic features for each specimen; revisions are listed on the right. Based on: Broili and Schöder (1936); Broom (1900, 1904a, 1904b, 1904c, 1904d, 1911, 1912, 1915, 1921, 1932); Cox (1964); Cox and Angielczyk (2015); Lydekker (1890); Owen (1876, 1879); Ray (2000); and Seeley (1892, 1894).

dimorphic (Sullivan et al., 2003) and this may be the case with *Endothiodon*, but because it is so commonly broken off, sexual dimorphism is difficult to determine (Macungo et al., 2019). The Mozambican sample also showed that the pineal boss is developed even in small individuals. Macungo et al. (2019) delved into the relationship between the number of tooth rows and condylobasal length of the skull, showing that it is not significant. This important finding has implications for revisions predating Cox (1964) where teeth were used as a species-level diagnostic character (Fig. 2). Furthermore, the thin sheet of dentary bone that covers some tooth rows medially (i.e. its absence giving the impression of multiple tooth rows) can be damaged or lost easily before burial and by later erosion, as shown in the Mozambican sample. Therefore, Macungo et al. (2019) concluded that the number of tooth rows is no longer a taxonomically viable character; we revisit this character here. Recently, Olroyd et al. (2021) supported this finding by histologically examining the multiple tooth rows of Mozambican *Endothiodon* as part of an investigation into the evolution of multiple tooth rows in dicynodonts.

Current consensus on *Endothiodon* diagnosis

The diagnostic cranial features of the genus *Endothiodon* include: deeply notched premaxilla; longitudinal snout ridges; moderately upturned dentary symphysis, often described as 'beak-like'; short secondary palate; prominent suborbital boss; a narrow intertemporal bar with a circular, oval or elongate pineal foramen sometimes situated on a robust pineal boss; a long and medially placed row of serrated teeth on the maxilla and dentary that can undergo multiple concomitant generations of tooth replacement throughout ontogeny (Boos et al., 2013; Cox & Angielczyk, 2015; Macungo et al., 2019; Olroyd et al., 2021; Ray, 2000). *Endothiodon* has been included in previous genus-level phylogenetic analyses of other dicynodonts (Angielczyk, 2001, 2007; Cluver & King, 1983; Cox & Angielczyk, 2015; Olroyd et al., 2017). Recently, phylogenetic analyses placed *Abajudon kaayai* in Endothiodontia, along with *Niassodon*, *E. tolani* and *E. bathystoma* (Angielczyk & Kammerer, 2017; Angielczyk et al., 2021; Macungo et al., 2023; Olroyd et al., 2017, 2021).

While *Endothiodon* is easily distinguishable from other dicynodonts, there have been no fine-scale phylogenetic analyses that encompassed multiple species and specimens that would discriminate all the species-defining features within the genus; thus, to date, there is no official consensus on the relationships within the genus *Endothiodon*. The currently accepted autapomorphies of *E. tolani* (described from Tanzania, Zambia and Mozambique) are a thin collar of bone surrounding the pineal foramen, instead of a well-developed pineal boss, and the presence of enlarged caniniforms (Cox & Angielczyk, 2015; Macungo et al., 2019). Meanwhile, autapomorphies of *E. mahalanobisi* (originally described from India) are a single broad snout ridge (as opposed to three), an elliptical pineal foramen on a low boss, and a relatively slender dentary (Ray, 2000). The third species, *E. bathystoma*, is known from south and east Africa, and Brazil (Boos et al., 2013; Macungo et al., 2019; this paper) and is distinguished by a robust pineal boss, a deeply vaulted premaxilla, more than one longitudinal snout ridge, and a robust dentary tapering anteriorly and extending upwards (Maharaj et al., 2021; Ray, 2000). However, many of the different species autapomorphies need to be assessed in a phylogenetic context, and some may be subject to confounding factors (e.g. the number of snout ridges, which may be influenced by lateral skull compression, and the robustness of the dentary, which may be an ontogenetic feature). The need for a review of the taxonomic features of *Endothiodon* is therefore paramount (Boos et al., 2013; Cox & Angielczyk, 2015; Macungo et al., 2019) especially as the Metangula Graben of Mozambique contains a mix of specimens with *E. tolani*-like and *E. bathystoma*-like features.

Institutional abbreviations

AMNH, American Museum of Natural History, New York, USA; **CGP**, Council for Geosciences, Pretoria, South Africa; **ISI**, Geology Museum, Indian Statistical Institute, Calcutta, India; **NHCC**, National Heritage Conservation Commission, Lusaka, Zambia; **NHMUK,** Natural History Museum, London, UK; **NMT**, National Museum of Tanzania, Dar es Salaam, Tanzania; **PPN**, Projecto PaleoMoz, Museu Nacional de Geologia, Mozambique; **SAM**, Iziko South African Museum, Cape Town, South Africa; **UEM**, Universidade Eduardo Mondlane, Maputo, Mozambique.

Materials and methods

We examined 150 *Endothiodon* specimens: their provenance, preserved portions and specimen numbers with their repositories are available in the Supplemental material Table S1. Photos of studied specimens, phylogenetic matrix, measurements and specimen coding are available in the Supplemental material.

Phylogenetic character descriptions and methods

We devised an entirely new phylogenetic matrix focused solely on resolving the taxonomy of *Endothiodon*.

Table 1. List of cranial specimens included in the phylogenetic analysis. **Abbreviations**: **CGS**, Council for Geosciences (Pretoria, South Africa); **ESI**, Evolutionary Studies Institute (Johannesburg, South Africa); **ISI**, Indian Statistical Institute (Kolkata, India); **NHCC**, National Heritage Conservation Commission (Lusaka, Zambia); **NHMUK**, Natural History Museum (London, United Kingdom); **NMT**, National Museum of Tanzania (Dar es Salaam, Tanzania); **PPN**, Museu Nacional de Geologia (Maputo, Mozambique); **SAM**, Iziko South African Museum (Cape Town, South Africa).

Taxon	Assigned species	Collection/reference
Outgroup 1	*Diictodon*	Macungo et al. (2023)
Outgroup 4	*Patranomodon*	Rubidge & Hopson (1995)
Outgroup 2	*Niassodon*	Castanhinha et al. (2013)
Outgroup 3	*Abajudon*	Olroyd et al. (2017)
ISIR 201	*E. mahalanobisi*	ISI; Ray (2000)
PPN2012-10-C3-1ß	*E. mahalanobisi*	PPN; Macungo et al. (2019)
NHCC LB 648	*E. tolani*	NHCC
NHCC LB 780	*E. mahalanonisi*	NHCC
NMT RB162	*E. tolani*	NMT
NMT RB475	*E. tolani*	NMT
BP/1/5505	*E. bathystoma*	ESI
NHMUK PV R4044	*E.* cf. *bathystoma*	NHMUK
NHMUK PV OR 49414	*E. bathystoma*	NHMUK
CGP/1/708	*Endothiodon bathystoma*	CGS
CGP/1/709	*E. bathystoma*	CGS
NHMUK PV R4042	*E. bathystoma*	NHMUK
NHMUK PV R1646	*E. bathystoma*	NHMUK; Owen (1876)
NHMUK PV R12443	*E. tolani*	NHMUK; Cox & Angielczyk (2015)
SAM-PK-2676	*E. bathystoma*	SAM
SAM-PK-K011271	*E. bathystoma*	SAM; Maharaj et al. (2021)
ISIR 202	*E. mahalanobisi*	ISI; Ray (2001)
BP/1/1659	*E. bathystoma*	ESI

We opted not to use any existing datasets because the anatomical detail required for a specimen-based data matrix to determine a genus-level tree necessitates the introduction of new characters. As such, we conducted a phylogenetic analysis focusing on intrarelationships of the genus *Endothiodon*. Out of the 150 specimens examined for anatomical variation, all the most common and taxonomically relevant characters were only present in 20 *Endothiodon* specimens: the remainder were substantially incomplete or not codable for more than nine characters. These 20 *Endothiodon* specimens also represent a sample of the best-preserved specimens assigned to *Endothiodon* in previous works, and were thus selected for the main phylogenetic analysis. When running the analysis, two wildcard operational taxonomic units (OTUs) were identified (CGP/1/689 and PPN2014-56) and removed using the command 'pcrprune', reducing the number of specimens to 18. Therefore, the total dataset used in this analysis contained 22 OTUs, consisting of 18 *Endothiodon* specimens and four outgroup taxa (*Diictodon feliceps*, *Niassodon mfumukasi*, *Abajudon kaayai* and *Patranomodon nyaphulii*), and 24 characters, seven of which are continuous while 17 are discrete (Table 1). We provide a tree with Bremer supports and symmetric resampling (Fig. 14A). We calculated Bremer supports from 4040 trees (cut 0) and relative Bremer supports from 839 trees (cut 0). We also calculated group frequencies after 10,000 replicates for symmetric resampling (P = 33) and GC values after 10,000 replicates for symmetric resampling (P = 33). The character matrix was constructed in Mesquite v. 3.70 (Maddison, 2008; Maddison & Maddison, 2021) and analysed in TNT v. 1.5, version of June 2021 (Goloboff & Catalano, 2016; Goloboff et al., 2008). Table 2 shows the list of cranial characters used.

All measurements for continuous characters (i.e. width, length, area, *etc*.) were taken using ImageJ v. 1.53e and then converted to a ratio (see the Supplemental material). A depiction of measurements is given in Figure 3. Measurements for each character were standardized across all specimens where the feature was preserved (i.e. to cancel out the units, by dividing by another skull measurement as in character 0, for example).

Character 0. Vomer size. Calculated as a ratio, by measuring the width (in mm across the widest point of the vomer) relative to the width of the maxilla. The width of the maxilla is the distance between the lateral edge of the tooth-bearing maxilla and the suture lateral to the palatine pads (Fig. 3A). Palatine pads are present often as deep depressions medial to the left and right maxillae.

Character 1. Area of the paired depressions on the palatine pads. Calculated as a ratio of the paired

Table 2. List of cranial characters included in the character matrix and their codes.

Region	Character	Code		
		0	**1**	**2**
Palate	**0**. vomer size (continuous)	–	–	–
Palate	**1**. palatine size (continuous)	–	–	–
Palate	**2**. upper tooth size (continuous)	–	–	–
Occiput	**3**. exoccipital condyle size (continuous)	–	–	–
Skull roof	**4**. pineal foramen size (continuous)	–	–	–
Dentary	**5**. dentary symphysis size (continuous)	–	–	–
Dentary	**6**. dentary tooth ratio (continuous)	–	–	–
Skull roof	**7**. pineal foramen shape	Oval	Circular	Narrow
Skull roof	**8**. pineal boss presence	Absent	Present	–
Skull roof	**9**. pineal boss shape	Robust	Thin collar	–
Palate	**10**. tusk presence	Absent	Present	–
Snout	**11**. snout crest presence	Absent	Present	–
Snout	**12**. snout crest shape	Shallow	Deep	–
Snout	**13**. snout shape	Round	Triangular	–
Palate	**14**. premaxilla excavation	Shallow	Deep	–
Palate	**15**. vomer position	Protruding	Hidden	–
Occiput	**16**. foramen magnum shape	Triangular	Circular	–
Occiput	**17**. opisthotic grooves	Absent	Present	–
Occiput	**18**. exoccipital condyle shape	Triangular	Irregular	–
Palate	**19**. palatine pads	Absent	Present	–
Skull roof	**20**. intertemporal bar	Wide	Narrow	–
Palate	**21**. upper tooth rows	Single	Multiple	–
Dentary	**22**. dentary tooth rows	Single	Multiple	–
Skull roof	**23**. prefrontal	Unswollen	Swollen	–

depressions on the palatine pad area (in mm^2) relative to the squared width of the maxilla (Fig. 3A). The paired depressions on the palatine pads varied considerably in size in undistorted specimens; thus, we included it as a continuous character.

Character 2. Maxillary tooth root size. Quantified as a ratio of average maxillary tooth root diameter relative to maxilla width. The variation in tooth size across *Endothiodon* specimens was quantified by measuring the average diameter (in mm) in a group of teeth in maxillae only. In this case, the teeth selected for measurement were from the fully erupted 'functional' row of larger teeth (i.e. along the line formed by the maxillary teeth cutting edge) and not the smaller, more posteriorly placed replacement teeth.

Character 3. Exoccipital condyle size. Measured as a ratio of exoccipital condyle area (in mm^2) (Fig. 3B) relative to the squared length from the snout tip to the anterior ramus of the pterygoid (Fig. 3C).

Character 4. Pineal foramen size. Calculated as a ratio of pineal foramen width (in mm: see Fig. 3D) relative to the length from the anterior snout tip to the anterior border of the pineal foramen. The pineal foramen width was measured laterally at the midpoint between its anterior and posterior borders.

Character 5. Dentary symphysis size. Measured as a ratio of height of the anterior tip of the symphysis relative to the width of the tooth-bearing portion of the dentary just posterior to the joining of the symphysis in dorsal view (Fig. 3E).

Character 6. Dentary tooth size. Quantified as a ratio of average dentary tooth diameter relative to dentary width (Fig. 3A).

Character 7. Pineal foramen shape is oval (0), circular (1) or narrow (2). An oval pineal foramen surrounded by a thin collar of bone is an autapomorphy of *E. tolani* (Cox & Angielczyk, 2015). This pineal foramen shape is distinct from the condition in *E. mahalanobisi* specimens ISIR 202 and ISIR 345 (the only specimens of that species with this feature preserved), which is far narrower and more slit-like. Although lateral compression of the skull can exaggerate the narrowness of the pineal foramen, the bone on which the narrow pineal foramen is situated in ISIR 345 is flat and undistorted (see the Supplemental material). Therefore, an 'oval' pineal foramen refers to the condition shown by *E. tolani* (NHMUK PV R12443), while a 'narrow' pineal foramen refers to that of *E. mahalanobisi* (ISIR 202) (Fig. 4A–C).

Character 8. Pineal boss is absent (0) or present (1).

Character 9. Pineal boss is robust (0) or a thin collar of bone surrounds the pineal foramen instead (1). *Endothiodon mahalanobisi* (ISIR 202) shows the condition of a pineal boss being completely absent and there are no signs of breakage in this region (Fig. 4). This differs from the thin collar of bone surrounding the pineal

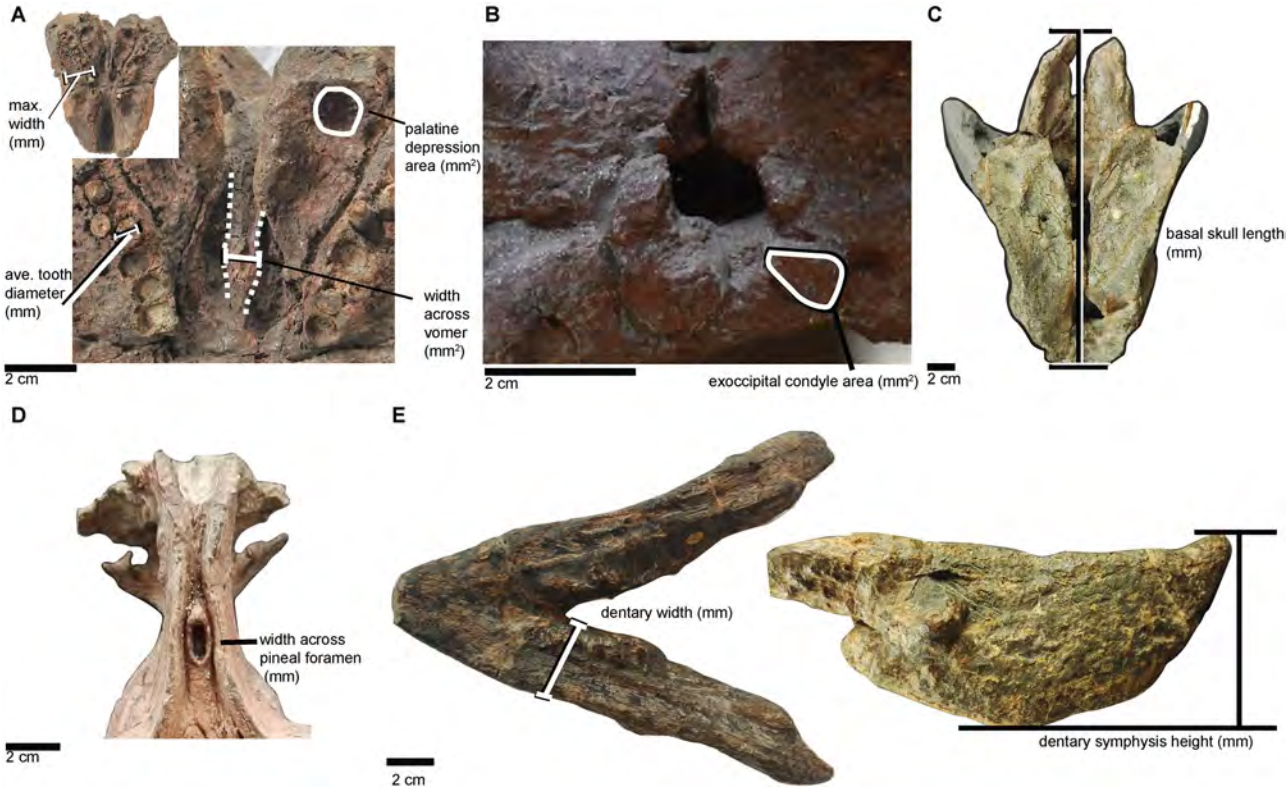

Figure 3. Measurements taken to quantify continuous features included in the phylogenetic analysis. **A**, measurement of average tooth diameter, vomer width, and palatine area, in *Endothiodon bathystoma* (NHMUK PV R4042, formerly '*E. uniseries*'). **B**, measurement of exoccipital area in *E. mahalanobisi* (ISIR 201). **C**, length from the anterior tip of the snout to the anterior ramus of the pterygoid in *Endothiodon* cf. *bathystoma* (NHMUK PV R4044, formerly '*E. uniseries*'). **D**, width across the pineal foramen in *E. tolani* (NHMUK PV R12443). **E**, dentary symphysis height and dentary width in NHMUK PV R4043.

foramen shown in some *E. tolani* specimens (e.g. NHMUK PV R12443). A robust pineal boss refers to the large round boss shown in an *E. bathystoma* specimen (SAM-PK-K-011271).

Character 10. Paired maxillary enlarged caniniforms are absent (0) or present (1). The presence of maxillary enlarged caniniforms (*sensu* Whitney et al., 2021) has so far been recorded only in *E. tolani* specimens (Fig. 5). Although they are usually small NMT RB 475 is the exception, having an unusually large tusk preserved (see Discussion). Because this is the only specimen in the present sample to do so, and because the large tusk is fragmented, it was not possible to accurately quantify this character; therefore, presence or absence is the only state regarding enlarged caniniforms in this study.

Character 11. Longitudinal snout crests are absent (0) or present (1). Previously, the number of snout crests or ridges was used in species diagnoses of *Endothiodon* (Ray, 2000); however, when examining the specimens, it was unclear what exactly a longitudinal snout crest was, or how to count them – as they could easily be confused with compaction-induced breakage and deformation along bone sutures. This feature can easily be affected by taphonomic deformation (see Discussion). However, if there are longitudinal crests on the premaxilla in undeformed skulls it should be apparent, but in laterally deformed skulls (e.g. Fig. 4G) the crests form distinct bulges separated by marked longitudinal grooves.

Character 12. Longitudinal snout crests are shallow (0) or prominent (1). Where snout crests are present, their depth is variable in undistorted specimens. Therefore, the presence and depth are here considered more reliable features than the number of crests (Fig. 4G, H).

Character 13. Dorsal snout shape is round (0) or triangular (1). In undistorted specimens of roughly similar sizes, the shape of the snout (containing premaxilla and nasals) in dorsal view differed from round to triangular, as shown in Figure 4D and E.

Character 14. In ventral view, the excavation of the premaxilla is shallow (0) or deep (1). The notched premaxilla in anterior view is a common feature of all *Endothiodon* specimens; however, the present sample contained variation in the depth of this excavation in ventral view, e.g. *E. bathystoma* (NHMUK PV R4042, formerly '*E. uniseries*') contains a deep premaxilla excavation, while *E. tolani* (NMT RB 475) has a

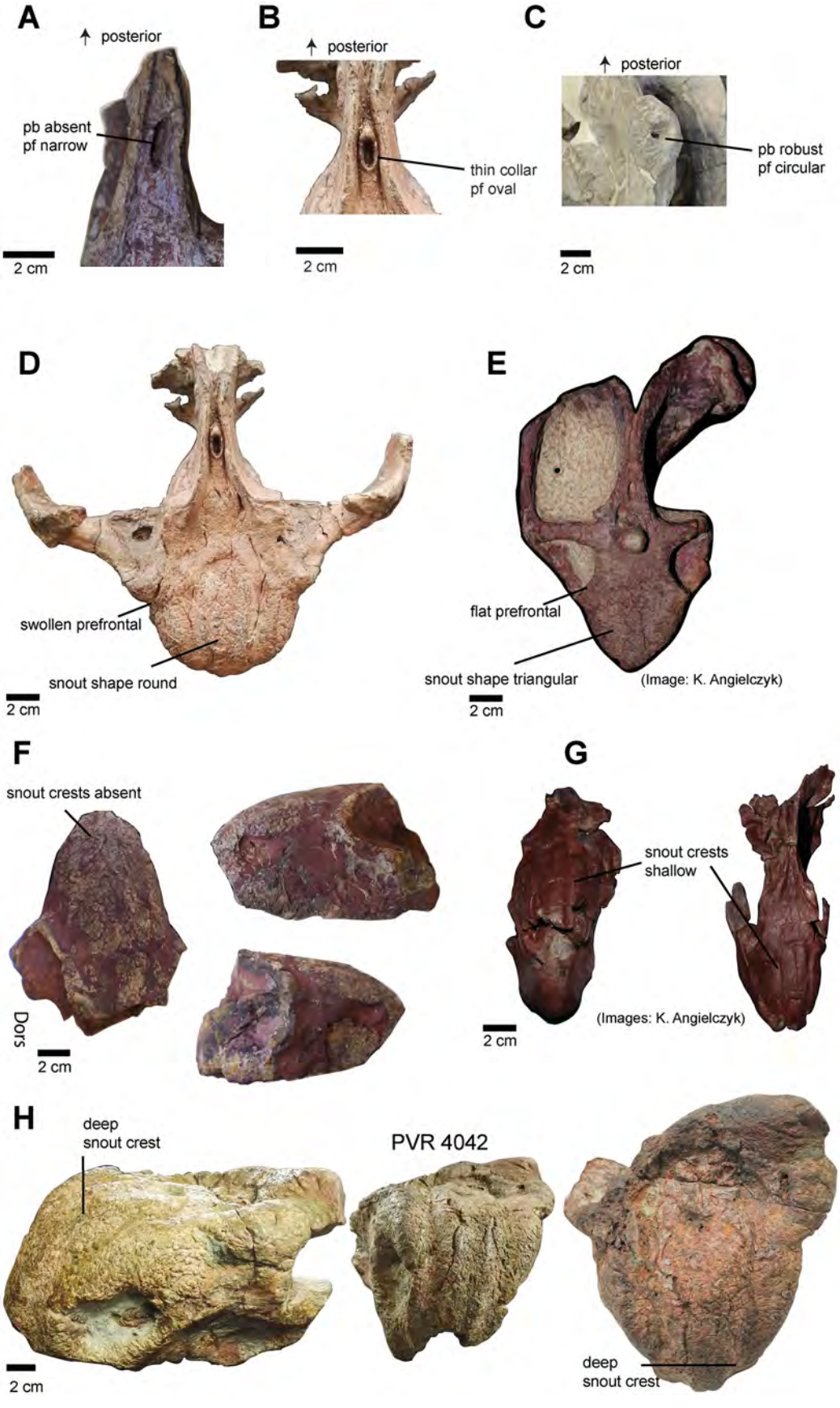
A
posterior
pb absent
pf narrow
2 cm
B
posterior
thin collar
pf oval
2 cm
C
posterior
pb robust
pf circular
2 cm
D
swollen prefrontal
snout shape round
2 cm
E
flat prefrontal
snout shape triangular
(Image: K. Angielczyk)
2 cm
F
snout crests absent
Dors
2 cm
G
snout crests
shallow
(Images: K. Angielczyk)
2 cm
H
deep
snout crest
PVR 4042
2 cm
deep
snout crest

shallow premaxilla excavation (Fig. 5). When coding this character, it is crucial to consider taphonomic processes that may impact it. Specifically, attention must be drawn to dorsoventral/lateral flattening and breakage of the premaxilla anteriorly. For example, NHMUK PV R4042 and NMT RB 475 both exhibit slight anterior breakage. However, NHMUK PV R4042 has a noticeably more notched excavation compared to the latter. Lateral flattening can also emphasize the depth of the ventral excavation. When there is substantial dorsoventral/lateral flattening there must be an effort to retrodeform the specimen to code it, otherwise it should be coded as '?'.

Character 15. Vomer protrudes ventrally at the level of the maxilla (0) or hidden deeper in the palate (1). In specimens where the palate is well preserved, the vomer is either hidden deeper in the palate or protruding, i.e. well exposed at the level of the ventral surface of the maxilla. *Endothiodon bathystona* (NHMUK PV R4042, formerly '*Endothiodon uniseries*') and *E. tolani* (NHMUK PV R12443) display these two states, respectively. These specimens are especially well prepared at the palatal region, so these two states are clearly anatomical and not due to differences in preparation quality.

Character 16. Foramen magnum is triangular (0) or circular (1). Contrast, for instance, the triangular foramen magnum of NHMUK PV R4044 and the circular foramen of ISIR 201. Particular caution must be taken when there is lateral compression or strong dorsoventral compression that could deform the walls of the foramen magnum (e.g. SAM-PK-K011271, SAM-PK-629). For those circumstances this character should be coded as '?'.

Character 17. Opisthotic bones are smooth (0) or have lateral 'folds' or grooves (1) on the posterior surface of the occipital plate. Interestingly, lateral 'folds' or grooves are present in the opisthotic bones of some *Endothiodon*. Although *E. mahalanobisi* (ISIR 201) is slightly dorsoventrally compressed (Fig. 6), these lateral opisthotic grooves are also present in other specimens and exist independently of distortion in *E. tolani* (NHCC LB 648 and NMT RB 162), *Endothiodon* sp. (CGP/1/708) and *E. bathystoma* (CGP/1/709 and BP/1/1659). In *Abajudon* the opisthotic grooves are subtriangular and bounded dorsally by pronounced crest, whereas in *Niassodon* they are absent.

Character 18. Exoccipital condyle is triangular (0) or bean-shaped (1). The shape of the exoccipital condyle varies between triangular and irregular, and this variation is observed regardless of specimen size (i.e. both smaller and larger skulls show both states). BP/1/1659 and NHCC LB 648 are examples of bean-shaped exoccipital condyles, whereas NHMUK PV R4044 has triangular exoccipital condyles (Fig. 6). Only well-preserved occipital condyles are considered, otherwise coded as '?' (e.g. ISIR 201). Indeed, this region of the skull is often subjected to erosion and damage.

Character 19. Paired depressions on palatine pads are absent (0) or present (1). Character to separate from outgroups, as these structures are known only in endothiodonts.

Character 20. Intertemporal bar is wide (e.g. *Cistecephalus*, *Abajudon*, *Niassodon*) (0) or narrow (e.g. *Endothiodon*) (1). Character to separate *Endothiodon* from other endothiodonts and outgroups. This character refers to the width of the interemporal bar strictly, not necessarily aspects of its construction such as the degree to which the postorbitals overlap the parietals, for instance.

Character 21. Maxillary teeth are present in single (0) or multiple (1) rows.

Character 22. Dentary teeth are present in single (0) or multiple (1) rows.

We test Macungo et al.'s (2019) hypothesis, and given further details on tooth row ontogeny provided by Olroyd et al. (2021), who has suggested that the number of tooth rows in the maxilla and dentary may not be taxonomically valid. However, the number of tooth rows has previously been used as a taxonomic feature for distinguishing *Endothiodon* species, with specimens previously assigned to *E. uniseries* having a single tooth row and other species having multiple rows (Owen, 1879). The number of tooth rows was here added as a character to test Macungo et al.'s (2019) hypothesis.

Character 23. Prefrontals are flat and unswollen (0) or swollen (1). This character was previously considered a distinguishing feature of *E. mahalanobisi* by Ray (2000), whereby the prefrontals were flat or unswollen in adult individuals of this species (Fig. 4). Swollen refers to a more robust and inflated prefrontal boss, whereas unswollen refers to a flat or unornamented prefrontal. The specimens in the current study indeed showed variation between unswollen prefrontals in

Figure 4. Examples of the different dorsal skull character states included in the phylogenetic analysis. **A**, the narrow pineal foramen of *Endothiodon mahalanobisi* (ISIR 201). **B**, the oval pineal foramen surrounded by a thin collar of bone in *E. tolani* (NHMUK PV R12443). **C**, the circular pineal foramen situated on a robust pineal boss in *E. bathystoma* (SAM-PK-K01127). **D**, round snout and swollen prefrontal of *E. tolani* (NHMUK PV R12443) compared to **E**, the triangular or pointed snout and unswollen prefrontals of *E. mahalanobisi* (NHCC LB 780). **F**, snout without longitudinal crests in *E. mahalanobisi* (ISIR 215). **G**, snout with shallow crests in *E. tolani*. (NMT RB162). **H**, deep snout crests in *E. bathystoma* (NHMUK PV R4042, formerly '*E. uniseries*'). **Abbreviations**: **pb**, pineal boss; **pf**, pineal foramen.

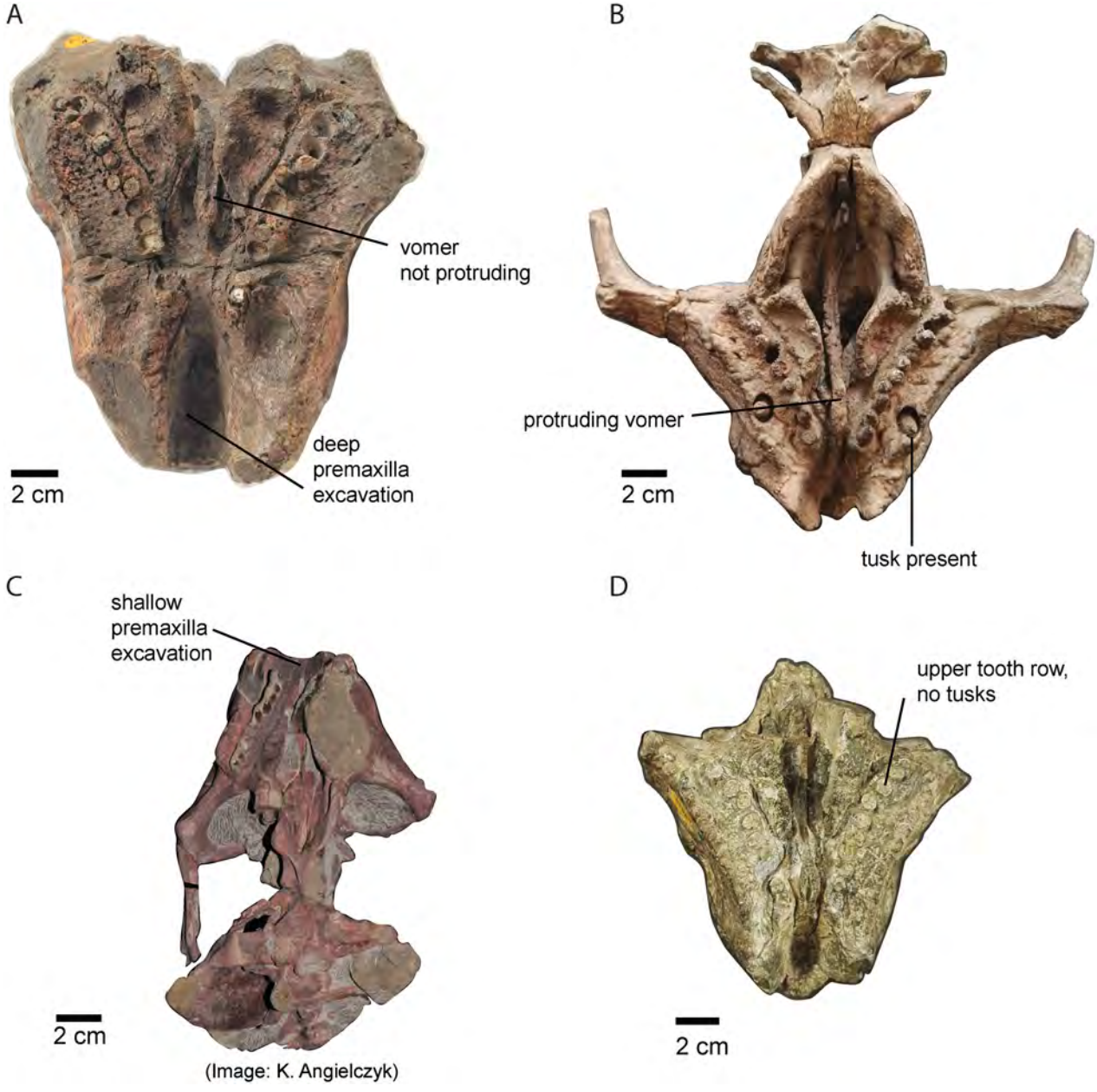

Figure 5. Examples of different palatal character states included in the phylogenetic analysis. **A**, *Endothiodon bathystoma* (NHMUK PV R4042, formerly '*E. uniseries*') has a vomer situated deeper in the palate, i.e. it does not protrude, and has a deep premaxilla excavation. In comparison, **B**, *E. tolani* (NHMUK PV R12443) has a protruding vomer; and **C**, *E. tolani* (NMT RB475) has a shallow premaxilla excavation. **D**, *E. tolani* (NHMUK PV R12443) has maxillary enlarged caniniforms in addition to teeth, while NHMUK PV OR49414 is tuskless.

E. mahalanobisi specimens and swollen prefrontals in others, e.g. *E. bathystoma.*

Stratigraphic placement of South African specimens

The revised litho- and biostratigraphic divisions of the Karoo Supergroup in South Africa (Day & Rubidge, 2020; Day & Smith, 2020; Rubidge et al., 2013; Smith, 2020; Smith et al., 2020) provided a framework that allowed for more accurate stratigraphic placement of South African *Endothiodon* specimens. By considering the geographical position of specimen localities and the distribution of vertebrate AZs and subzones, the stratigraphic placement of South African Karoo specimens (Table 3) was determined. Each subzone corresponds to a stratigraphic column at the type locality, allowing the relative positions of *Endothiodon* specimens to be

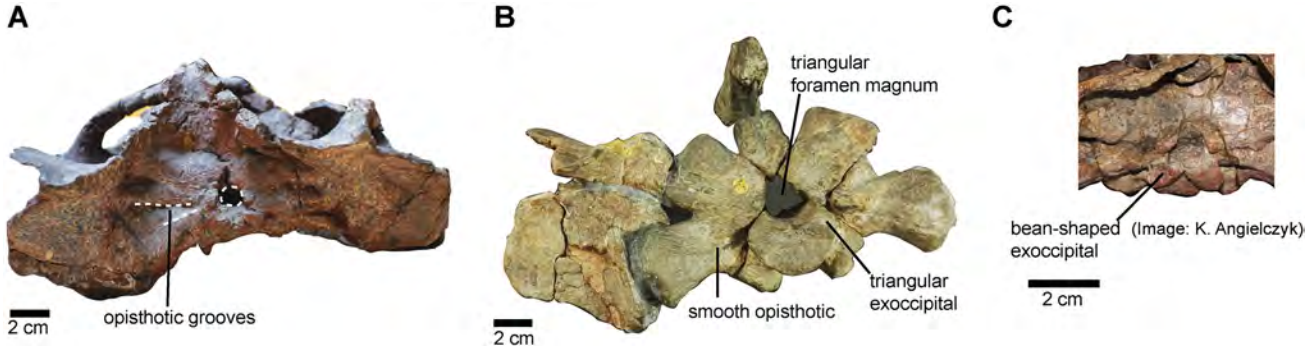

Figure 6. Examples of different occipital character states included in the phylogenetic analysis. **A**, *Endothiodon mahalanobisi* (ISIR 201) has a circular foramen magnum, and lateral grooves on both opisthotic bones. **B**, *Endothiodon* cf. *bathystoma* (NHMUK PV R4044, formerly '*E. uniseries*') has a more triangular foramen magnum, smooth opisthotic bones and triangular exoccipital condyles. **C**, this contrasts with the irregular exoccipitals shown in *Endothiodon* cf. *bathystoma* (NHCC LB 648).

determined (Day & Rubidge, 2020; Day & Smith, 2020; Smith, 2020; Smith et al., 2020). Geographical maps with pinned coordinates of specimen localities were overlaid with biozonation maps to identify the corresponding biozone. However, due to incomplete geographical data in some of the collection databases, there is uncertainty regarding the exact stratigraphic position of these specimens (M. Day, pers. comm., 2021). Once allocated to an approximate stratigraphic level, the specimens were associated with the corresponding biozone (Fig. 7) and radiometric dates (Rubidge et al., 2013; Smith et al., 2020).

Results

Endothiodon anatomy of main Karoo Basin specimens and biostratigraphy

In our study of South African main Karoo Basin *Endothiodon* specimens, their abundance, broad stratigraphic range and historical significance make them a benchmark for comparison. The examination includes a detailed analysis of specimen ages and a comprehensive description of skull features from pivotal specimens (Fig. 7). Our prioritization of the anatomical review and biostratigraphy of South African specimens is grounded in several justifications. Firstly, our confirmation that only *E. bathystoma* is present in South Africa holds crucial palaeobiogeographical implications. This finding suggests a palaeo-west to palaeo-east gradient of *Endothiodon* species, enriching our understanding of the species distribution (see Discussion). Secondly, verification that *Endothiodon* is exclusively confined to the *Endothiodon* AZ reinforces existing knowledge. Although not groundbreaking, a thorough revision of all relevant specimens serves as a significant test of the most recent biostratigraphic revisions (Day & Smith, 2020), contributing to the robustness of these findings. Thirdly, our confirmation that *Endothiodon tolani* and *E. mahalanobisi* are absent in South Africa adds clarity to the regional composition of the genus (see Discussion). This observation refines our understanding of the palaeogeographical distribution of *Endothiodon* species. Moreover, our investigation into the morphology of *E. bathystoma* in South Africa reveals a remarkable consistency over time. Crucial diagnostic characters identifying *E. bathystoma* exhibit no significant variation across various subzones, which are details we examined closely. The South African *Endothiodon* specimens, constituting the largest collection of the genus globally, house the best-preserved and most complete examples. This collection represents a crucial initial step in the comprehensive study of the genus, providing a valuable resource for further research. Lastly, to enhance the precision of our findings, we included in Table 3 the level of stratigraphic precision for each specimen. Despite variability between historic specimens and those collected under modern criteria, this addition contributes to a more nuanced understanding of the specimens' stratigraphic context. The phylogenetic analysis results retrieved all South African specimens as a single clade. All 27 specimens fall into the *Endothiodon* AZ (Fig. 7). No specimens, even those with the vaguest locality data, could be confidently placed in the re-defined *Cistecephalus* AZ. Additional stratigraphic details on the *Endothiodon* specimens are available in the Supplemental material.

Lower *Lycosuchus-Eunotosaurus* Subzone. CGP/1/687 is a partial dentary of *E. bathystoma* with teeth arranged in multiple rows (Fig. 8A). The average tooth diameter ratio is 0.19, and its dentary symphysis height ratio is 2.43. SAM-PK-K1682 is an *Endothiodon* sp. laterally compressed maxilla fragment. The teeth have an average

Table 3. List of *Endothiodon* specimens known from the South African Karoo Basin described and included in the stratigraphic context. 'No subzone details' refers to specimens that could not be narrowed down to a subzone. Geographic/stratigraphic location precision: level 1 – global positioning system coordinates recorded at time of collection and stratigraphic position plotted on measured section with field notes; level 2 – coordinates taken from labelled dot marked on a field map plus field notes; level 3 – coordinates of centroid point of farm on which the specimen was collected and determined by collection manager; level 4 – no coordinates for locality, specimen collected without recording a farm name and only a region or district recorded.

Assemblage zone	Subzone	Specimen	Previously assigned	Geographic/stratigraphic location precision level
Endothiodon	General *Tropidostoma-Gorgonops*	NHMUK PV OR 49414 (NHMUK PV R8173 cast of NHMUK PV OR 49414)	*E. bathystoma*	4
		NHMUK PV OR 49415	*E. bathystoma*	4
	Lower *Tropidostoma-Gorgonops*	CGP/1/T2	*Endothiodon* sp.	2
		NHMUK PV R4042	*E. bathystoma*	3
		NHMUK PV R4043	*E. bathystoma*	3
		NHMUK PV R4044	*E.* cf. *bathystoma*	3
	Lowermost *Tropidostoma-Gorgonops* / Uppermost *Lycosuchus-Eunotosaurus*	CGP/1/709	*E. bathystoma*	2
		CGP/1/782	*Endothiodon bathystoma*	2
		SAM-PK-K6727	Endothiodontia indet.	1
	Upper *Lycosuchus-Eunotosaurus*	CGP/1/708	*Endothiodon bathystoma*	2
		SAM-PK-628	*E. bathystoma*	3
		SAM-PK-629	*E. bathystoma*	3
		SAM-PK-2676	*E. uniseries*	3
		SAM-PK-K011271	*E. bathystoma*	1
		SAM-PK-K11221	*E. bathystoma*	1
		SAM-PK-K11131	*E. bathystoma*	1
		SAM-PK-K11134	*E. bathystoma*	1
	General *Lycosuchus-Eunotosaurus*	NHMUK PV OR 49394	*E. bathystoma*	3
		NHMUK PV OR 49397	*E. bathystoma*	3
		NHMUK PV R7866	Endothiodontia indet.	3
		SAM-PK-3420	*Endothiodon* sp.	3
		SAM-PK-3442	Endothiodontia indet.	3
		SAM-PK-5605	*Endothiodon* sp.	3
		CGP/1/777	*E. bathystoma*	2
	Lower *Lycosuchus-Eunotosaurus*	CGP/1/687	*E. bathystoma*	2
		SAM-PK-K1682	Endothiodontia indet.	1

diameter of 6.8 mm (Fig. 8B). There are no tusked South African *Endothiodon* specimens.

Upper *Lycosuchus-Eunotosaurus* Subzone. CGP/1/708 is the upper portion of a large *Endothiodon* sp. skull featuring a robust pineal boss with a circular pineal foramen. Exact tooth row count is indeterminate and enlarged caniniforms are absent. The snout has a low medial crest, a rounded anterior shape and a shallow premaxilla excavation (Fig. 9A). In occipital view, a circular foramen magnum and opisthotic grooves can be seen. SAM-PK-628 is an *E. bathystoma* dentary with a fused dentary symphysis (height ratio 3.62) and a dentary tooth ratio of 0.18. SAM-PK-629 is a weathered *E. bathystoma* skull with plaster reconstructed squamosals and devoid of enlarged caniniforms but has a shallow premaxillary excavation, a round snout and a prominent medial crest (Fig. 9B, C). SAM- PK-2676, formerly assigned to '*E. uniseries*', is an incomplete *E. bathystoma* skull with maxillary teeth measuring an average 5.91 mm (Fig. 9D).

SAM-PK-K11131 is a large *E. bathystoma* skull and dentary with preserved teeth, no enlarged caniniforms and well-fused sutures. Its attached dentary has a strongly co-ossified symphysis leaving no suture visible and a weathered sulcus, along with other features

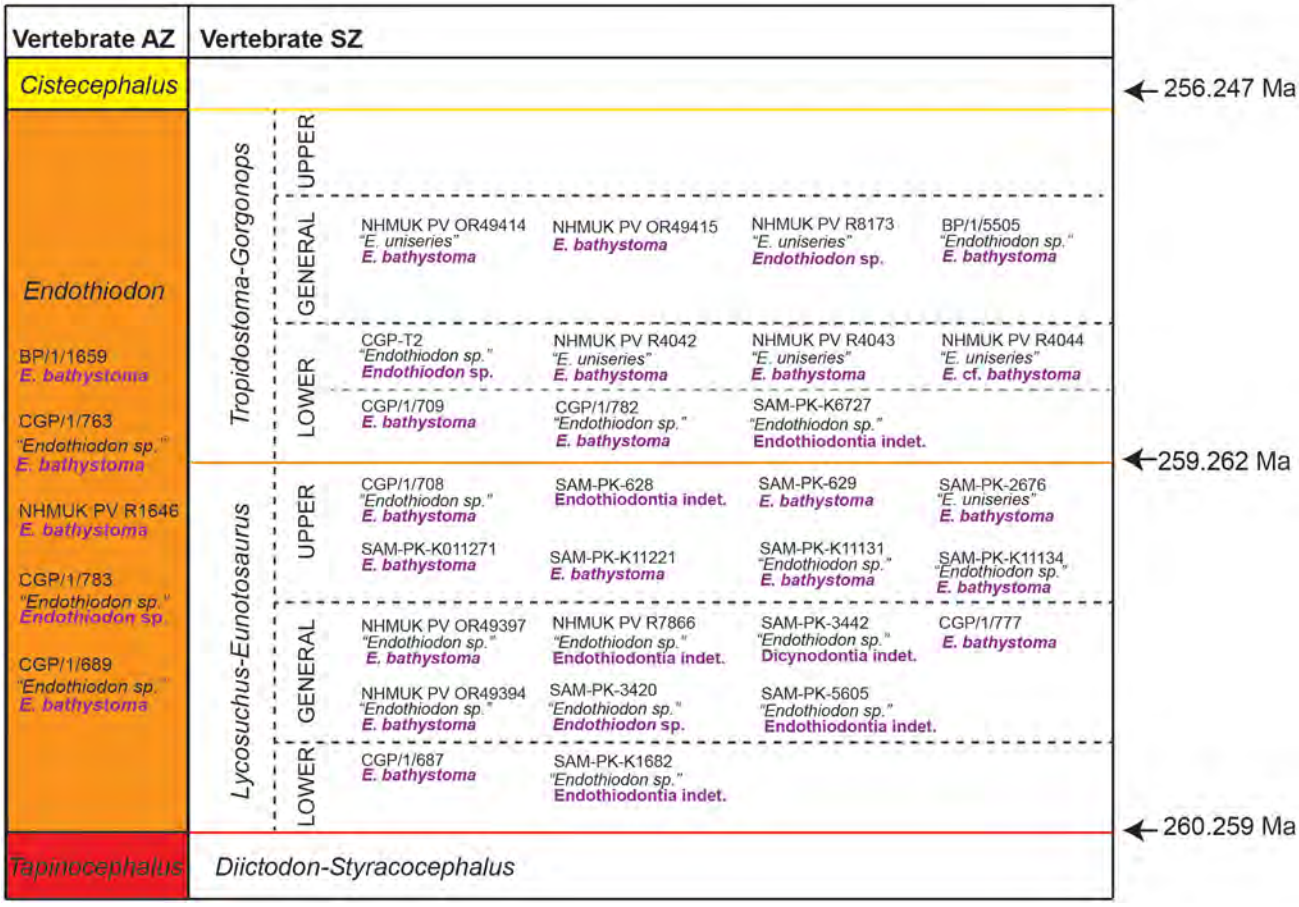

Figure 7. Chart showing the approximate stratigraphic placement to subzone level of South African *Endothiodon* specimens from the Karoo Basin, modified from Smith et al. (2020, table 1) to include specimens from this study. Radiometric dates on the right are taken from Rubidge et al. (2013) and Smith et al. (2020). The specimens placed in the 'general' region of the subzones could not be placed more specifically within the subzone (i.e. could not be assigned to either the upper or the lower region). Specimens BP/1/1659, CGP/1/763, NHMUK PV R1646 (holotype of *E. bathystoma*), *Endothiodon* sp. CGP/1/783 and *E. bathystoma* CGP/1/689 could not be placed into a subzone within the *Endothiodon* assemblage zone. NHMUK PV OR 49414 was previously assigned as the holotype of '*E. uniseries*'. The genus and species identity of specimens in the figure are written as per their previous assignments in the literature or in museum collection databases. The purple text indicates their revised assignments. **Abbreviations**: **AZ**, assemblage zone; **SZ**, subzone.

like a narrow mandibular fenestra, lateral dentary swelling and a fused prearticular-articular complex. The dentary symphysis ratio is 2.99, dentary tooth ratio is 0.02. SAM-PK-K11134 is a well-preserved *E. bathystoma* dentary with a strongly co-ossified symphysis leaving no suture visible (height ratio 3.39), extended sulcus, lateral shelf, narrow fenestra, some serrated teeth and a fused prearticular-articular complex (Fig. 9E). The dentary tooth ratio is 0.16 (Fig. 9F). SAM-PK-K11221 is a broken *E. bathystoma* dentary with symphysis height ratio of 1.91 and dentary tooth ratio of 0.18 (Fig. 9G). SAM-PK-K011271 is a complete *E. bathystoma* skull (Maharaj et al., 2021) with maxillary teeth obscured by the mandible and a dentary teeth ratio of 0.15. The dentary symphysis height ratio is 3.78 (Fig. 9H).

General *Lycosuchus-Eunotosaurus* Subzone. The term 'general subzone' is used when precise stratigraphic position within subzones is not recorded. CGP/1/777 is an *E. bathystoma* anterior dentary fragment with preserved tooth rows and a strongly co-ossified symphysis leaving no suture visible; its estimated height ratio is 2.95 and its dentary tooth ratio is 0.22 (Fig. 10A). NHMUK PV R7866 is a fused Endothiodontia indet. dentary symphysis, while NHMUK PV OR49394 is a weathered right palate of *E. bathystoma* with preserved maxillary teeth but without enlarged caniniforms.

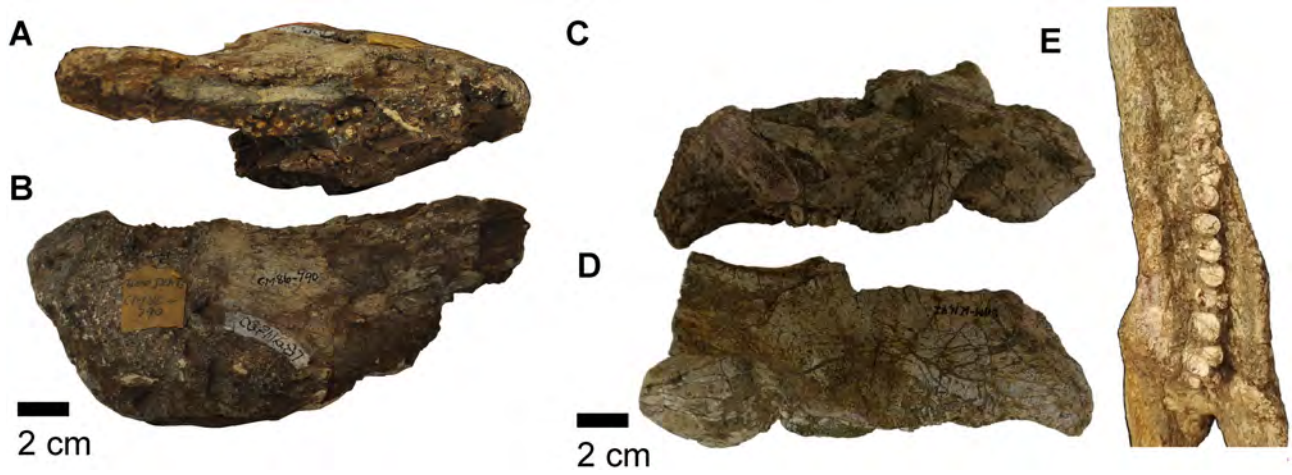

Figure 8. *Endothiodon* specimens from the lower *Lycosuchus-Eunotosaurus* Subzone. **A**, CGP/1/687 a partial dentary of *E. bathystoma* in dorsal and **B**, lateral view. SAM-PK-K1682, Endothiodontia indet. maxilla fragment in **C**, medial, **D**, lateral, and **E**, ventral views.

NHMUK PV OR49397 is a weathered *E. bathystoma* dentary fragment, partially preserving the tooth row and having a symphysis tip height ratio of 1.98 and dentary tooth ratio of 0.25 (Fig. 10B, C, D). SAM-PK-3420 is an *Endothiodon* sp. skull anterior portion with multiple rows of maxillary teeth, a rounded snout with prominent medial crest and a deep excavation of the premaxilla. SAM-PK-5605 are *Endothiodon* dentary fragments, with the latter displaying a lateral swelling, lateral dentary shelf and a fused prearticular-articular complex (Fig. 10E, F, G).

Lower *Tropidostoma-Gorgonops* Subzone. CGP-T2 is an incomplete *Endothiodon* sp. palate and snout with a deep premaxilla excavation and maxillary tooth diameter averaging 5.0 mm (Fig. 11A). CGP/1/709 is a large *E. bathystoma* skull and dentary with features including: prominent snout crest and a rounded anterior snout shape, no enlarged caniniforms, potential multiple maxillary tooth rows, circular pineal foramen with a pronounced pineal boss, protruding vomer, circular foramen magnum, presence of a dentary lateral swelling and a robust basioccipital. Dentary symphysis and tooth ratios are 3.06 and 0.17, respectively (Fig. 11B). CGP/1/782 is an *E. bathystoma* dentary anterior portion with strongly co-ossified symphysis leaving no suture visible between the dentaries and splenials, with a dentary symphysis ratio of 3.99 and a dentary tooth ratio of 0.19 (Fig. 11C). NHMUK PV R4042 is an *E. bathystoma* robust anterior snout and palate with multiple tooth rows but no enlarged caniniforms (Fig. 11E–G). Interestingly, a deep notch-like depression is visible just posterior to the right ventral premaxilla projection, wrongly called a 'caniniform process' by Cox (1964). The snout medial crest is prominent, the snout shape is rounded and it has a deep ventral excavation of the premaxilla. The vomer does not protrude to the level of the maxilla (Fig. 11D). NHMUK PV R4043 is an *E. bathystoma* anterior dentary with dentary symphysis and tooth ratios of 3.29 and 0.19, respectively (Fig. 11E). NHMUK PV R4044 is another *Endothiodon* cf. *bathystoma* skull and dentary, with dentary symphysis and tooth ratios of 3.89 and 0.23, respectively (Fig. 11F). The snout is rounded with three prominent snout crests, and the premaxilla excavation is shallow. The vomer protrudes at maxilla level. In occipital view, the foramen magnum is triangular and the opisthotic bones are smooth and lack grooves. The mandibular fenestra is narrow and the splenials are fused. The reflected lamina of the angular is not flared. SAM-PK-K6727 is a small Endothiodontia indet. dentary fragment with some preserved teeth and an estimated, yet potentially deformed, dentary tooth ratio of 0.22 (Fig. 11G).

General *Tropidostoma-Gorgonops* Subzone. NHMUK PV R8173 is a cast of *Endothiodon* sp. basicranial material featuring a robust basioccipital and grooved opisthotic (Fig. 12A). The associated NHMUK PV OR49414 lacks enlarged caniniforms but has a single row of teeth and a triangular snout with a prominent medial crest (Fig. 12B). NHMUK PV OR49415 is an *E. bathystoma* anterior dentary with strongly co-ossified symphysis leaving no suture visible between dentaries and splenials, a dentary symphysis ratio of 3.51, and a dentary tooth ratio of 0.19 (Fig. 12C).

Other specimens in the *Endothiodon* AZ. CGP/1/689, a laterally compressed *E. bathystoma* skull, features a circular pineal foramen on a robust pineal boss, no enlarged caniniforms, two prominent snout crests, a triangular snout and a robust vomer protruding at the

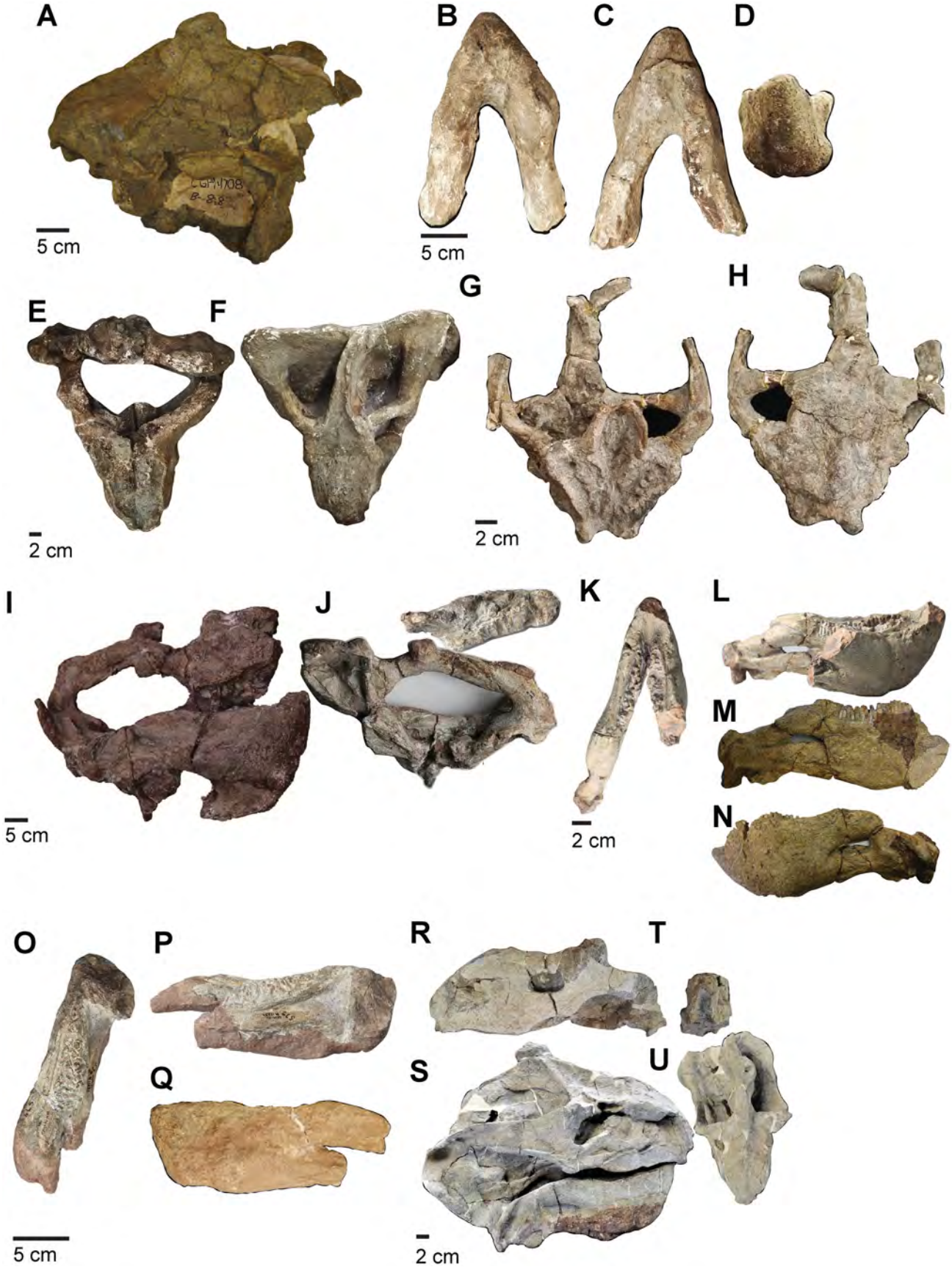
A
B
C
D
5 cm
5 cm
E
F
G
H
2 cm
2 cm
I
J
K
L
M
N
5 cm
2 cm
O
P
Q
R
T
S
U
5 cm
2 cm

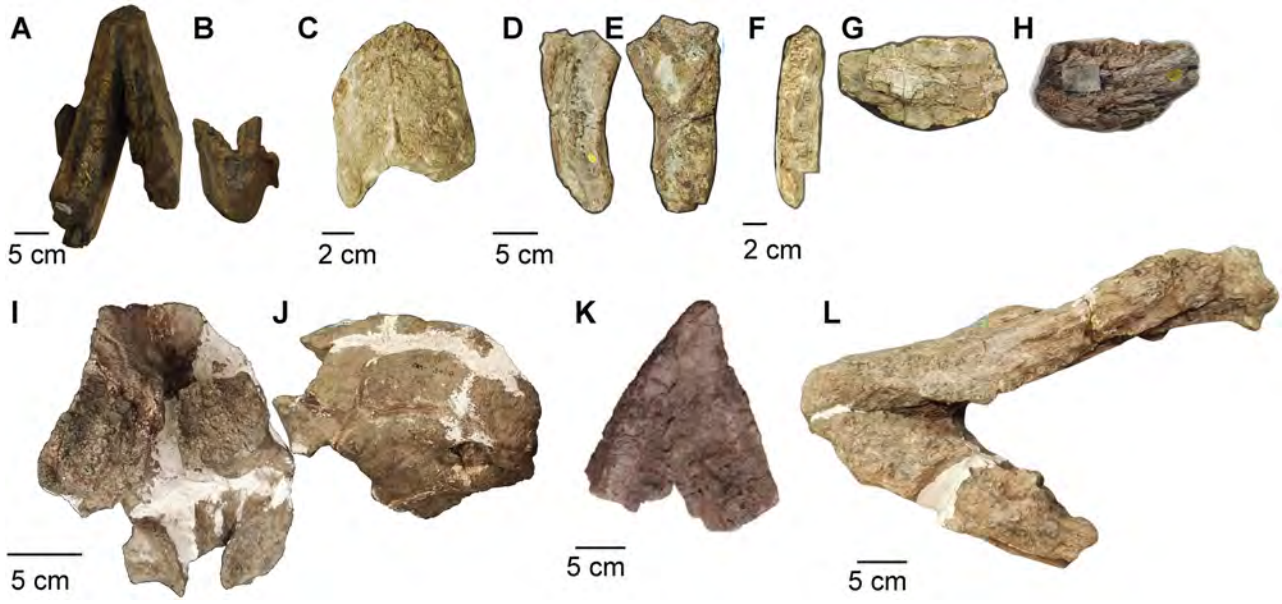

Figure 10. *Endothiodon* specimens from the *Lycosuchus-Eunotosaurus* Subzone that could not be accurately positioned stratigraphically within the subzone (i.e. upper or lower). CGP/1/777, an *E. bathystoma* dentary fragment in **A**, dorsal and **B**, anterior views. NHMUK PV R7866, an Endothiodontia indet. partial dentary, **C**, in anterior view. NHMUK PV OR 49394, an *E. bathystoma* partial maxilla in **D**, ventral and **E**, dorsal views. NHMUK PV OR 49397, an *E. bathystoma* weathered dentary fragment in **F**, dorsal, **G**, right lateral, and **H**, right medial views. SAM-PK-3420, an *Endothiodon* sp. anterior snout and palate in **I**, ventral and **J**, right lateral views. **K**, SAM-PK-3442, a Dicynodontia indet. fragment previously attributed to '*Endothiodon* sp.' **L**, SAM-PK-5605, an Endothiodontia indet. partial dentary in dorsal view.

maxilla level, with bone breaks near the sutures (Fig. 13A). CGP/1/673, an *E. bathystoma* partial dentary fragment with dentary tooth and symphysis height ratios of 0.22 and 3.55, respectively (Fig. 13B). Subzone specification was not feasible for these specimens.

Phylogenetic analysis

To generate the most parsimonious tree, the FUSE algorithm was used in one tree retained after ~99 million re-arrangements; with a tree length of 41.680, a consistency index of 0.513, and a retention index of 0.702. The phylogenetic analysis retrieved three main groups: two mostly dominated by specimens previously ascribed to *E. mahalanobisi* and *E. tolani* (more basal) and one clade mostly dominated by specimens previously ascribed to *E. bathystoma* and *E. uniseries*.

***Endothiodon mahalanobisi* clade.** Clade A is considered here the species concept for *Endothiodon mahalanobisi* as it includes the holotype of this species (ISIR 201) and specimens more closely related to it than to any other *Endothiodon* specimen. The *E. mahalanobisi* clade, shown in green in Figure 14B, contains tuskless specimens (in contrast to the tusked *E. tolani*) with an oval or narrow pineal foramen with no pineal boss (in contrast to *E. bathystoma* which has a circular pineal foramen on a robust boss) nor any collar of bone surrounding the pineal foramen (in contrast to *E. tolani*); as well as flat/unswollen prefrontals (in contrast to swollen prefrontals in all other species). The *E. mahalanobisi* clade is united by the presence of a triangular exoccipital condyle shape (ch. 18) and represents the *E. mahalanobisi*-like morphotype. Figure 15 shows a comparison of specimens in this clade, and a summary of shared features is given in Table 4. The specimen previously assigned to *E. mahalanobisi* (ISIR 201) is a complete skull whereby the dentary is not separated from the skull, and the pineal foramen is not preserved; therefore,

Figure 9. *Endothiodon* specimens from the upper *Lycosuchus-Eunotosaurus* Subzone. **A**, CGP/1/708, an *E. bathystoma* skull in left lateral view. SAM-PK-628, dentary of Endothiodontia indet. in **B**, ventral, **C**, dorsal, **D**, anterior views. SAM-PK-629, skull of *E. bathystoma* in **E**, ventral, **F**, dorsal views. SAM-PK-2676, *E. bathystoma* skull previously assigned to '*E. uniseries*' in **G**, ventral and **H**, dorsal views. SAM-PK-11131, an *E. bathystoma* partial skull in **I**, right lateral and **J**, ventral views. SAM-PK-K11134, an *E. bathystoma* partial dentary in **K**, dorsal, **L**, right lateral, **M**, medial and **N**, left lateral views. SAM-PK-K11221, *E. bathystoma* partial left dentary in **O**, dorsal, **P**, right lateral and **Q**, left lateral views. SAM-PK-K011271, complete skull of *E. bathystoma* in **R**, left lateral, **S**, right lateral, **T** anterior and **U**, dorsal views.

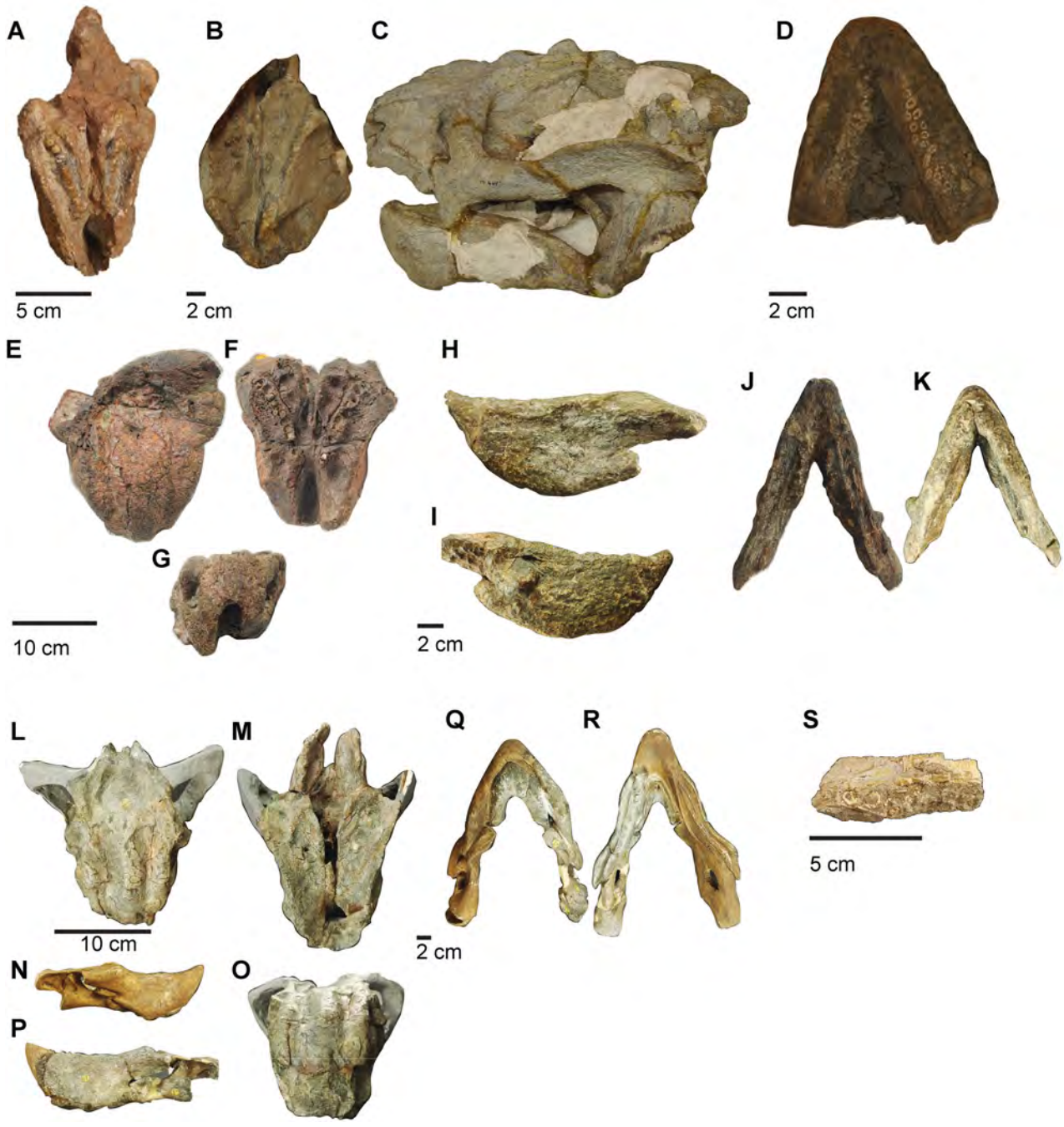

Figure 11. *Endothiodon* specimens from the lower *Tropidostoma-Gorgonops* Subzone. **A**, CGP-T2, an *Endothiodon* sp. partial snout and maxilla in ventral view. CGP/1/709, an *E. bathystoma* skull and dentary in **B**, ventral and **C**, left lateral views. **D**, CGP/1/782, an *E. bathystoma* partial anterior dentary in dorsal view. NHMUK PV R4042, a partial *E. bathystoma* snout and palate previously assigned to '*E. uniseries*' in **E**, dorsal, **F**, ventral, and **G**, anterior views. NHMUK PV R4043, an *E. bathystoma* dentary previously assigned to '*E. uniseries*' in **H**, left lateral, **I**, right lateral, **J**, dorsal and **K**, ventral views. *Endothiodon* cf. *bathystoma*, NHMUK PV R4044, and dentary previously assigned to '*E. uniseries*' with incomplete skull in **L**, dorsal and **M**, ventral views, **N**, mandible in right lateral view, **O**, skull in anterior view, and mandible in **P**, left lateral, **Q**, ventral and **R**, dorsal views. **S**, SAM-PK-K6727, Endothiodontia indet., a weathered dentary fragment in dorsal view.

it can only be coded for the occipital and dorsal snout regions. Its exoccipital condyle shape is triangular (ch. 18), and its snout shape is round (ch. 13). Furthermore, the prefrontals in this specimen are flat and unswollen (ch. 23). ISIR 202 is a tuskless anterior snout with a palate that preserves phylogenetically codable

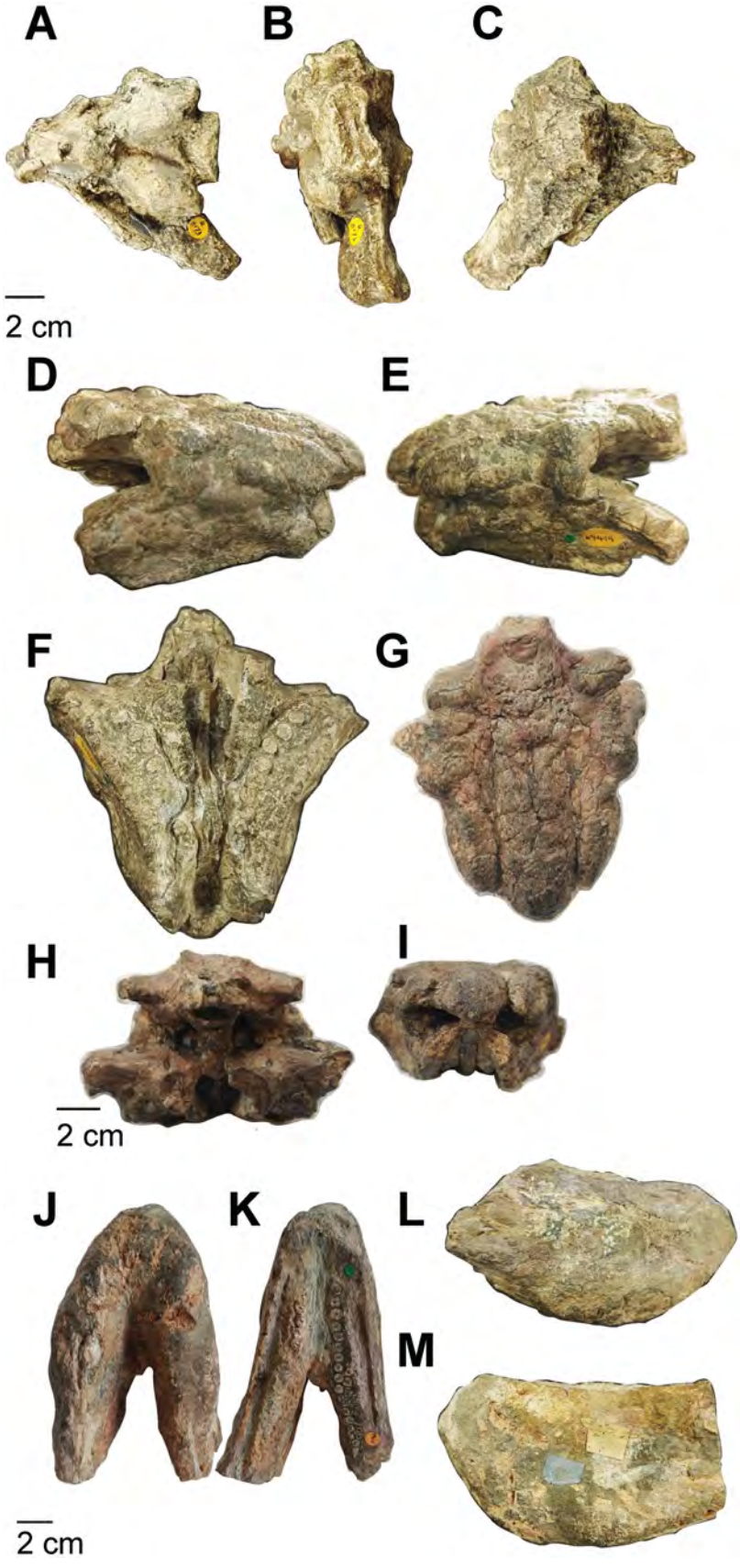
A
B
C
2 cm
D
E
F
G
H
I
2 cm
J
K
L
M
2 cm

Figure 13. *Endothiodon* specimens from the *Endothiodon* Assemblage zone that could not be allocated to a subzone. CGP/1/689, *E. bathystoma* partial anterior skull in **A**, left lateral and **B**, ventral views. CGP/1/673, *E. bathystoma* partial mandible in **C**, right lateral and **D**, dorsal views.

information and has a triangular snout shape (ch. 10 and 13). This specimen also has unswollen prefrontals (ch. 23). NHCC LB780 belongs to this clade because it is also tuskless (ch. 10) and has an oval pineal foramen, although it is unclear whether it was surrounded by the typical *E. tolani*-like collar of bone (ch. 7 and 9). NHCC LB 780 was probably overprepared in the pineal foramen region. Its exoccipital condyle shape (ch. 18) is triangular; it has unswollen prefrontals (ch. 23) and a triangular snout shape. PPN2012-10-C3-1ß was previously assigned as *E. bathystoma* due to the absence of enlarged caniniforms (ch. 10); however, the phylogenetic analysis places it in the *E. mahalanobisi*-like clade. It is united with NHCC LB 780 and ISIR 202 by its triangular snout (ch. 13) and unswollen prefrontals (ch. 23).

In this clade the only specimen with a rounded snout shape is ISIR 201, but this specimen is dorsoventrally compressed. A triangular exoccipital condyle shape (ch. 18) is present in ISIR 201 and NHCC LB 780, but this feature is not preserved in other specimens. NHCC LB 780, ISIR 202 and PPN2012-10-C3-1ß are tuskless (see ch. 10 as a uniting feature of B1, the tusked group), and united by a triangular snout shape (ch. 13). ISIR 202 and PPN2012-10-C3-1ß are further united by vomer size (ch. 0), pineal foramen size (ch. 4), and a non-protruding vomer (ch. 15). PPN2012-10-C3-1ß, NHCC LB 780, ISIR 201 and ISIR 202 have flat/unswollen prefrontals (ch. 23). In contrast, all the other specimens (where preserved) are united by swollen prefrontals, i.e. they appear slightly bulbous, especially in anterior and lateral views. NHCC LB 780 (Zambia) and ISIR 202 (India) are also approximately the same size as the other *E. tolani* specimens (Tanzania, i.e. NMT RB162, NHMUK PV R12443 and NMT RB475). They also have similar dimensions. PPN2012-10-C3-1ß (Mozambique) and ISIR 201 (India) are similar in size to each other (and slightly larger than NHCC LB 780 and ISIR 202); however, all they have in common with each other are low, weakly defined snout crests (ch. 12). Note that ISIR 201 does not expose palatal features so it cannot be accurately compared to ISIR 202.

Clade *E. tolani* + E. *bathystoma*.

1. *E. tolani* clade (B1). The most parsimonious tree retrieves a clade (Clade B1, blue in Fig. 14) formed by specimens previously ascribed to *E. tolani*, namely: NMT RB162, NHMUK PV R12443 and NMT RB475 (Fig. 16). Clade B1 is considered here

Figure 12. *Endothiodon* specimens from the *Tropidostoma-Gorgonops* Subzone that could not be accurately positioned stratigraphically within the subzone. *Endothiodon* sp. (NHMUK PV R8173), a cast of a basicranium fragment previously assigned to '*E. uniseries*' in **A**, ventral, **B**, posterior and **C**, dorsal views. *E. bathystoma* (NHMUK PV OR49414), an anterior snout and palate previously assigned to '*E. uniseries*' in **D**, right lateral, **E**, left lateral, **F**, ventral, **G**, dorsal, **H**, posterior and **I**, anterior views. *E. bathystoma* (NHMUK PV OR49415), an anterior dentary previously assigned to '*E. uniseries*' in **J**, ventral, **K**, dorsal, **L**, right lateral and **M**, left lateral views.

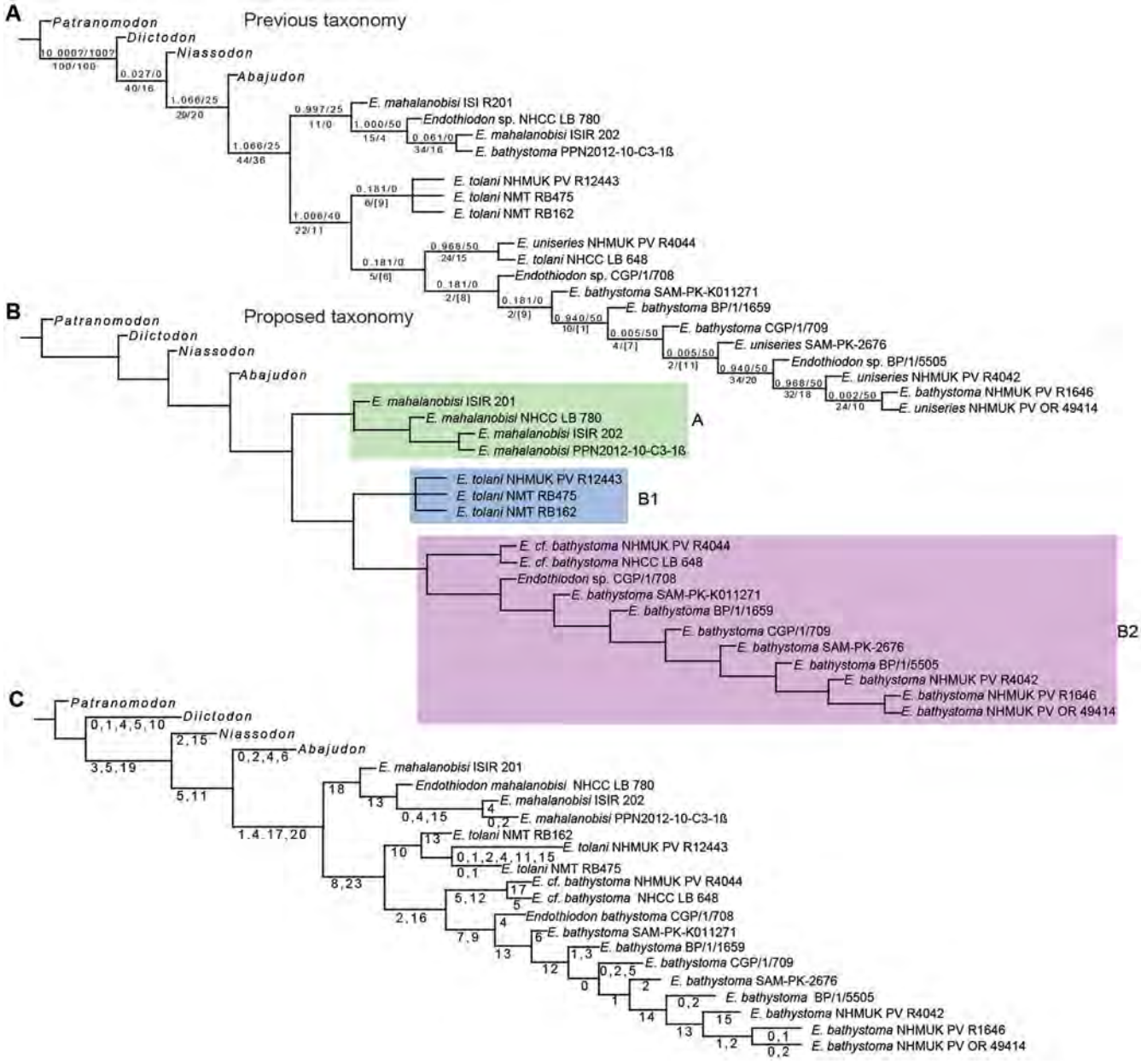

Figure 14. Most parsimonious tree showing phylogenetic intrarelationships of *Endothiodon* specimens within the genus. **A**, tree with Bremer supports and symmetric resampling. Values above branches are Bremer supports (from 4040 trees, cut 0)/Relative Bremer supports (from 839 trees, cut 0). Values below branches are group frequencies after 10,000 replicates, cut 50 (tree 0) for symmetric resampling (P = 33)/GC values after 10,000 replicates, cut 0 for symmetric resampling (P = 33). **B**, modified version of '**A**' to highlight three main clades recovered in *Endothiodon*. Clade A (green) contains two specimens previously ascribed to *E. mahalanobisi*, one specimen previously ascribed to *E. bathystoma*, and one *Endothiodon* sp. specimen; Clade B consists of B1 (blue) containing specimens previously ascribed to *E. tolani*, and B2 (purple) with specimens previously ascribed to *E. bathystoma* and *E. uniseries*. **C**, synapomorphies common to each specimen from the character list (characters beneath branches).

the species *Endothiodon tolani* as it includes the holotype specimen (NHMUK PV R12443) and specimens more closely related to it than to any other *Endothiodon* specimen. They are united by the presence of enlarged caniniforms (ch. 10), which separates them from the other *Endothiodon* specimens in this analysis. Clade B1 is separated from the *E. mahalanobisi* clade (Clade A) by the presence of a collar of bone surrounding the oval pineal foramen (ch. 9) and swollen prefrontals (ch. 23). NHMUK PV R12443 is an almost complete skull with palate exposed to reveal enlarged

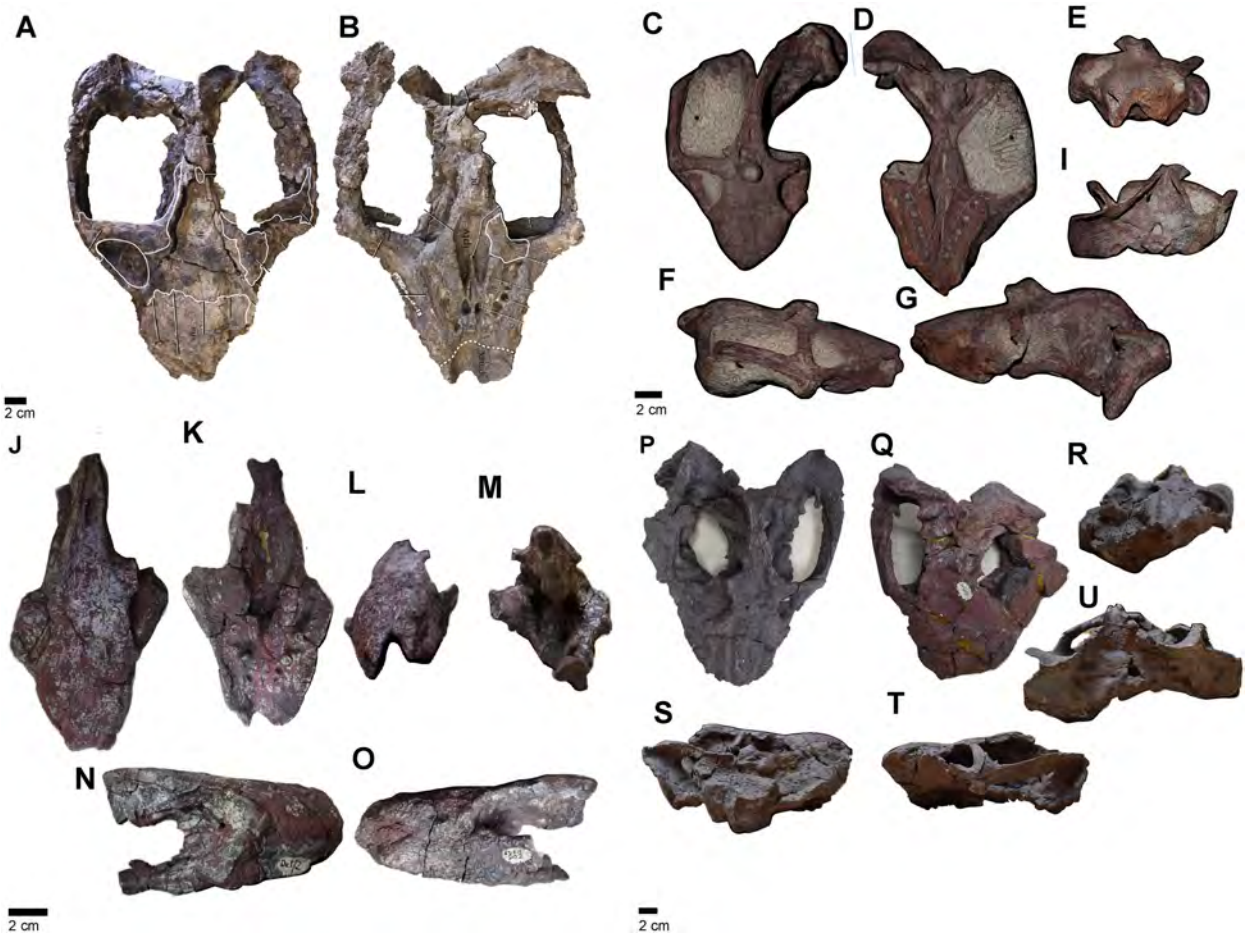

Figure 15. Comparison of skulls in clade A of the phylogenetic analysis. Formerly *Endothiodon bathystoma* PPN2012-10-C3-1ß, now *E. mahalanobisi*, in **A**, dorsal and **B**, ventral views. NHCC LB 780, *E. mahalanobisi* in **C**, dorsal, **D**, ventral, **E**, anterior, **F**, right lateral, **G**, left lateral, and **I**, posterior views. ISIR 202, *E. mahalanobisi* snout and palate in **J**, dorsal, **K**, ventral, **L**, anterior, **M**, posterior, **N**, right lateral, and **O**, left lateral views. ISIR 201, *E. mahalanobisi* skull in **P**, dorsal, **Q**, ventral, **R**, anterior, **S**, right lateral, **T**, left lateral and **U**, posterior views.

caniniforms (ch. 10). It is morphologically similar to NMT RB475 and the phylogenetic analysis retrieved them in the same clade. Although the maxillae and dentaries of NMT RB162 are not separated, a partial tusk is visible on the left lateral side of this specimen. This skull is separated from the other two *E. tolani* specimens based on its snout shape (ch. 13), but this difference is likely due to lateral compression of the skull. Table 5 depicts the morphological differences between the clade here proposed to represent *E. tolani* and *E. bathystoma*.

2. *E. bathystoma* clade (B2). Clade B2 is considered here the *Endothiodon bathystoma* clade as it includes the holotype of this species (NHMUK PV R1646) and specimens more closely related to it than to any other *Endothiodon* specimen. The holotype of *E. uniseries* (NHMUK PV OR49414) also belongs to this clade, but *E. bathystoma* has nomenclatural priority. The recovered *E. bathystoma* (Clade B2, purple, Fig. 14) is distinct from the *E. tolani* clade based on maxillary tooth size (ch. 2) and foramen magnum shape (ch. 16). The formerly classified *E. uniseries* NHMUK PV R4044 and *E. tolani* NHCC LB 648 are retrieved in a cluster because they share the presence of prominent snout crests (ch. 12) and similar dentary symphysis size (ch. 5), but neither seems to have a pineal foramen and boss preserved (see the Supplemental material). Some reservations, however, need to be considered as the pineal foramen region in these specimens is damaged. Additionally, no palatal information is visible for NHCC LB 648 as the dentary and maxilla are not separated to reveal the presence of enlarged caniniforms, but computed tomography scan (CT) data indicates they are present. However, NHMUK PV R4044 and NHCC LB 648 are also united to other *E. bathystoma* by maxillary

Table 4. Comparison of shared anatomical features among skulls placed in clade A of the phylogenetic analysis. Features that were not preserved were coded as '?'.

Feature	PPN2012-10-C3-1ß	NHCC LB 780	ISIR 201	ISIR 202
Pineal foramen shape	?	Oval	?	Narrow
Pineal boss	Absent	Absent	?	Absent
Enlarged caniniforms	Absent	Absent	?	Absent
Snout crests	Shallow	Absent	Shallow	Absent
Snout shape	Triangular	Triangular	Circular	Triangular
Premaxilla excavation	Shallow	Shallow	?	Shallow
Vomer protrusion	Exposed	Not exposed	?	Exposed
Foramen magnum shape	?	Triangular	Circular	?
Opisthotic	?	Groove	Groove	?
Exoccipital condyle shape	?	Triangular	Triangular	?
Maxillary tooth row	Single	Single	?	Single
Prefrontal	Flat	Flat	Flat	Flat

tooth size (ch. 2) and foramen magnum shape (ch. 16) (Fig. 17). The remainder of specimens comprising the *E. bathystoma* clade is a mix of formerly classified *E. bathystoma*, *E. uniseries* and *Endothiodon* sp. specimens, and they all have preserved a circular pineal foramen (ch. 7) and robust pineal boss (ch. 9).

The three main groups in the phylogenetic analysis support the hypothesis that *Endothiodon* contains three species: *E. mahalanobisi* (ISIR 201 and ISIR 202 from India; NHCC LB 780 from Zambia; and PPN2012-10-C3- 1ß from Mozambique); *E. tolani* (NMT RB 162, NMT RB 475 and NHMUK PV R12443 from Tanzania); and *E. bathystoma* (BP/1/5505, BP/1/1659, CGP/1/708, CGP/1/709, NHMUK PV R1646, NHMUK PV R4042, NHMUK PV OR 9414, SAM-PK-2676 and SAM-PK-K011271).

Systematic palaeontology

Therapsida Broom, 1904d
Anomodontia Owen, 1860
Dicynodontia Owen, 1859
Endothiodontia Owen, 1876
Endothiodon Owen, 1876

Type species. *Endothiodon bathystoma* Owen, 1876.

Revised generic diagnosis. Updated from Cox and Angielczyk (2015), combining data from Olroyd et al. (2018, 2021) and Castanhinha et al. (2013). Medium to large dicynodont with more than seven maxillary and post-canine dentary teeth, notched anterior end of the premaxilla and a corresponding fitting upturned beak of the dentaries, absence of caniniform process, with paired depressions on palatine pads. The premaxillary and maxillary teeth are medially located and there is a shelf-like area lateral to the maxillary non-caniniform teeth. Similarly, the dentary teeth are located medially, potentially presenting multiple tooth rows. The maxillary and dentary teeth present coarse serrations. As in some emydopoids, the posterior dentary sulcus is narrow and deep and extends posterior to the dentary teeth. The intertemporal bar is narrow. The pineal foramen is located at approximately mid-length of the intertemporal bar. The transverse flange of the pterygoid is short. In terms of autapomorphies *Endothiodon* has a marked posteroventrally directed boss on the jugal in the ventral-most point of the postorbital bar and the dorsal surface of the snout has longitudinal crests; also, it has a highly angular junction of the suborbital bar with the zygomatic arch (where both structures are subequal in width, *contra Cistecephalus*).

Differential diagnosis. *Niassodon* can be differentiated from *Endothiodon* by having a smoothly rounded zygomatic arch confluent with the suborbital bar, absence of opisthotic grooves, absence of longitudinal crests, having a broad intertemporal bar, and having a radiating pattern of grooves and ridges on the dorsal surface of the frontals. *Abajudon* can be differentiated from *Endothiodon* by the absence of cingulated teeth, the absence of corrugations on the teeth, having a smoothly rounded zygomatic arch confluent with the suborbital bar, the absence of opisthotic grooves, the absence of longitudinal crests, and having a broad intertemporal bar.

Note on synonymy list. We follow Matthews (1973).

Endothiodon bathystoma Owen, 1876

(Figs 1, 3A, E, 4C, H, 5A, 6B, 8A, B, 9, 10A, B, D–H, 11B–G, 12D–M, 13, 16I–O)

v* 1876 *Endothiodon bathystoma* Owen: 66, pls 66, 67.
v 1879 *Endothiodon uniseries* Owen: 557, pl. 27.

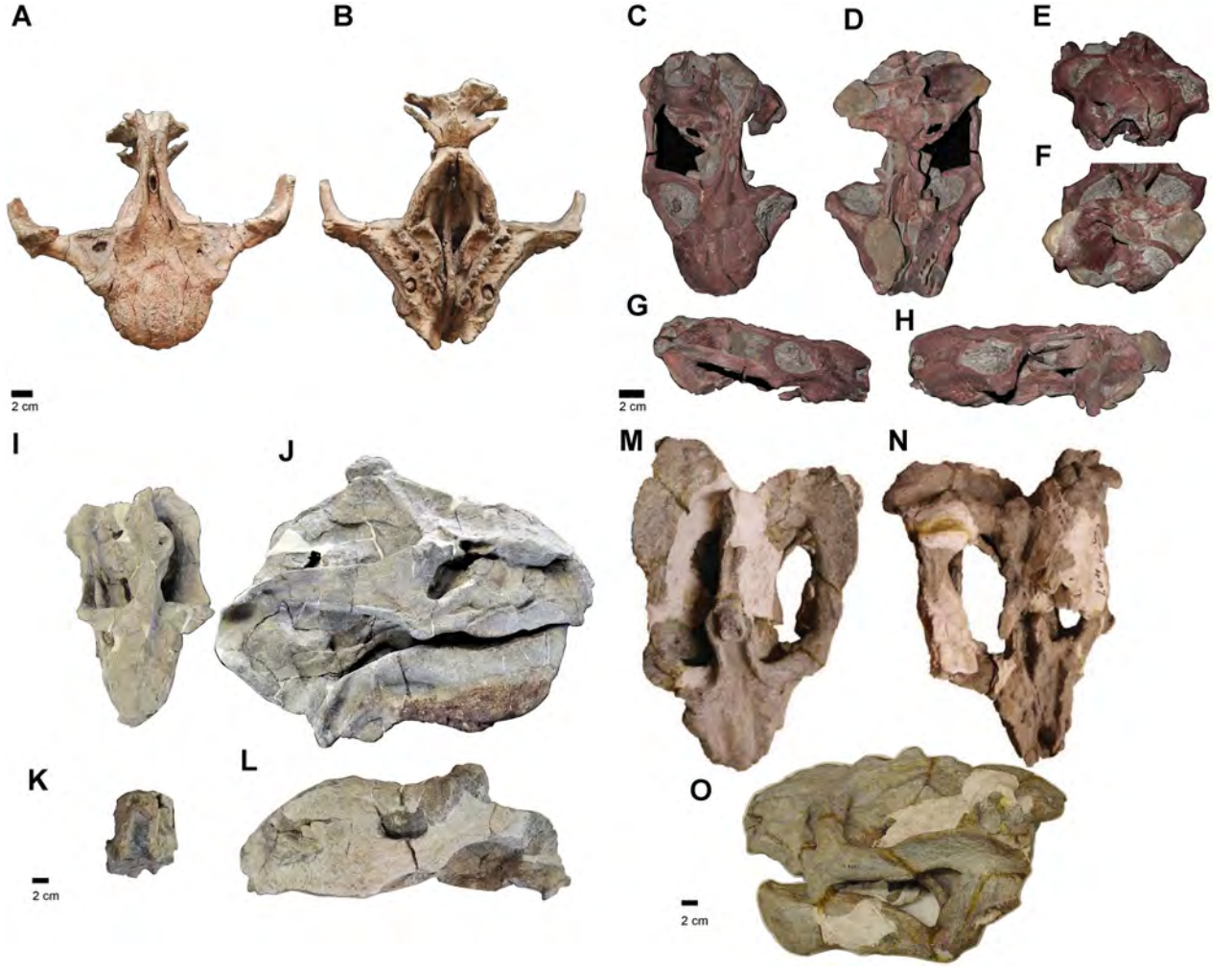

Figure 16. Comparison of skulls in clade B of the phylogenetic analysis to confirm the distinction between *Endothiodon tolani* and *E. bathystoma* specimens. NHMUK PV R12443, *E. tolani* skull in **A**, dorsal and **B**, ventral views. NMT RB475, *E. tolani* in **C**, dorsal, **D**, ventral, **E**, anterior, **F**, right lateral, **G**, right lateral, and **H**, left lateral views. SAM-PK- K011271, *E. bathystoma* skull in **I**, dorsal, **J**, right lateral, **K**, anterior, and **L**, left lateral views. CGP/1/709, *E. bathystoma* in **M**, dorsal, **N**, ventral, and **O**, left lateral views.

v 1890 *Endothiodon microps* (Owen); Lydekker: 66 (*partim*).
v 1894 *Esoterodon uniseries* (Owen): Seeley: 1001.
v 1904c *Prodicynodon pearstonensis*: Broom: 70; pl. 4, fig. 3, 4.
v 1904c *Opisthoctenodon agilis*: Broom: 71; pl. 4, fig. 1.
v 1904d *Chelyoposaurus williamsi* Broom: 184.
v 1912 *Esoterodon whaitsi* Broom: 866.
v 1912 *Endothiodon platyceps* Broom: 867.
v 1912 *Emydochampsa platyceps* Broom: 875.
v 1915 *Endothiodon paucidens* Broom: 148, fig. 39 (*partim*).
v 1915 *Endothiodon seeleyi* Broom: 149.
v 1915 *Endothiodon platyceps* (Broom): Broom: 150, fig. 40 (*partim*).
v 1915 *Endothiodon whaitsi* (Broom): Broom: 154, fig. 43.
v 1921 *Endothiodon crassus* Broom: 672, fig. 45.
v 1923 *Endothiodon angusticeps* Broom: 682, fig. 15.
v 1932 *Pachytegos stockleyi* Haughton: 650, figs 12, 13.
v 1932 *Esoterodon angusticeps* (Broom); Broom: 234, figs 76D, E, 77, 78B.
v 1932 *Esoterodon paucidens* (Broom); Broom: 237, figs 76A, 78, 79D.
v 1932 *Endogomphodon minor* Broom: 239, fig. 79B.
v 1936 *Emydochampsa oweni* Broili and Schöder: 22, figs 1–5.

Holotype. NHMUK PV R1646, partial skull and dentary.

Referred specimens. BP/1/1659, BP/1/5443, BPI/1/5470, BPI/1/5491, BPI/1/5492, BPI/1/5498, BP/1/5505, BP/1/7267, CGP/1/687, CGP/1/689, CGP/1/708, CGP/1/709, CGP/1/763, CGP/1/777, CGP/1/782, NHMUK PV

Table 5. Differences in features between specimens assigned to the *Endothiodon tolani* clade and those assigned to the *E. bathystoma* clade in the phylogenetic analysis. Features that were not preserved were coded as '?'.

Specimen	NHMUK PV R12443	NMT RB475	SAM-PK-K011271	CGP/1/709	NHCC LB 648	NHMUK-PV-4044
Species	*E. tolani*	*E. tolani*	*E. bathystoma*	*E. bathystoma*	*E. tolani*	*E.* cf. *bathystoma*
Pineal foramen shape	Oval	Oval	Circular	Circular	Oval	?
Pineal boss	Thin collar	Thin collar	Robust	Robust	Thin collar	?
Tusk	Present	Present	Absent	Absent	?	Absent
Snout crest	Absent	Shallow	Shallow	Deep	Deep	Deep
Snout shape	Circular	Circular	Triangular	Triangular	Circular	Circular
Premaxilla excavation	Shallow	Shallow	Shallow	Shallow	?	Shallow
Vomer protrusion	Exposed	Hidden	?	Hidden	?	Hidden
Foramen magnum shape	Circular	?	?	Triangular	Triangular	Triangular
Opisthotic	?	?	?	?	Groove	Absent
Exoccipital condyle shape	?	Irregular	?	Irregular	Irregular	Irregular
Maxillary tooth row	Single	Single	?	Single	?	Single
Dentary tooth row	Single	?	?	Multiple	?	Single
Prefrontal	Swollen	Swollen	Swollen	Swollen	Swollen	Swollen

R1969, NHMUK PV R4042, NHMUK PV R4043, NHMUK PV OR 49394, NHMUK PV OR49397, NHMUK OR49414, NHMUK PV OR49415, SAM-PK-588, SAM-PK-629, SAM-PK-2676, SAM-PK-7252, SAM-PK-10150, SAM-PK-10638, SAM-PK-10642, SAM-PK-K11131, SAM-PK-11134, SAM-PK-K11221, SAM-PK-K011271, UEM 01, UEM 107, UEM 36-61, UEM 24-61, NHMUK R 36708, BP/1/7067, AMNH FARB 5257, AMNH FARB 5516, AMNH FARB 5565, ANHM FARB 5570, ANHM FARB 5571, AMNH FARB 5572, AMNH FARB 5612, AMNH FARB 5615, PV 0226P, ISIR 204, ISIR 206, PPN2014-23, PPN2014-70-2, PPN2014-70-3, PPN2014-70-6D, PPN2014-70-6d.

***Endothiodon* cf. *bathystoma*.** AMNH FARB 5614, NHMUK PV R4044 and NHCC LB 648 (Figs 3C, 6B, C, 11L–R, 17).

Emended diagnosis. *Endothiodon* species with the following autapomorphies: a circular pineal foramen situated on a robust pineal boss, along with the absence of enlarged caniniforms and swollen prefrontals. Labial migration of functional marginal teeth, leaving trails of alveolar bone, sometimes resulting in multiple tooth rows. The following combination of characters is diagnostic of *Endothiodon bathystoma:* circular pineal foramen on a robust pineal boss, absence of enlarged caniniforms, swollen prefrontals, pronounced snout crests.

Endothiodon mahalanobisi Ray, 2000

(Figs 3B, 4A, E, F, 6A, 15)

Holotype. ISIR 201, an almost complete skull and dentary.

Referred specimens. ISIR 202, PPN2012-10-C3-1ß, NHCC LB 780.

Emended diagnosis. *Endothiodon* species with the following autapomorphies: a narrow/oval pineal foramen on an unornamented surface with no pineal boss or collar of bone; low or absent snout crests; the absence of enlarged caniniforms; single tooth row; and flat unswollen prefrontals.

***Endothiodon* cf. *mahalanobisi*.** ISIR 213, ISIR 214, ISIR 215, ISIR 220, ISIR 341, ISIR 364 (due to presence of three low snout crests, premaxillary notch and unswollen prefrontals), ISIR 245 (due to absence of pineal boss but also narrow and unornamented pineal foramen).

Endothiodon tolani Cox and Angielczyk, 2015

(Figs 3D, 4B, D, G, 5B, C, D, 6C, 16–H)

Holotype. NHMUK PV R12443, a partial skull and dentary.

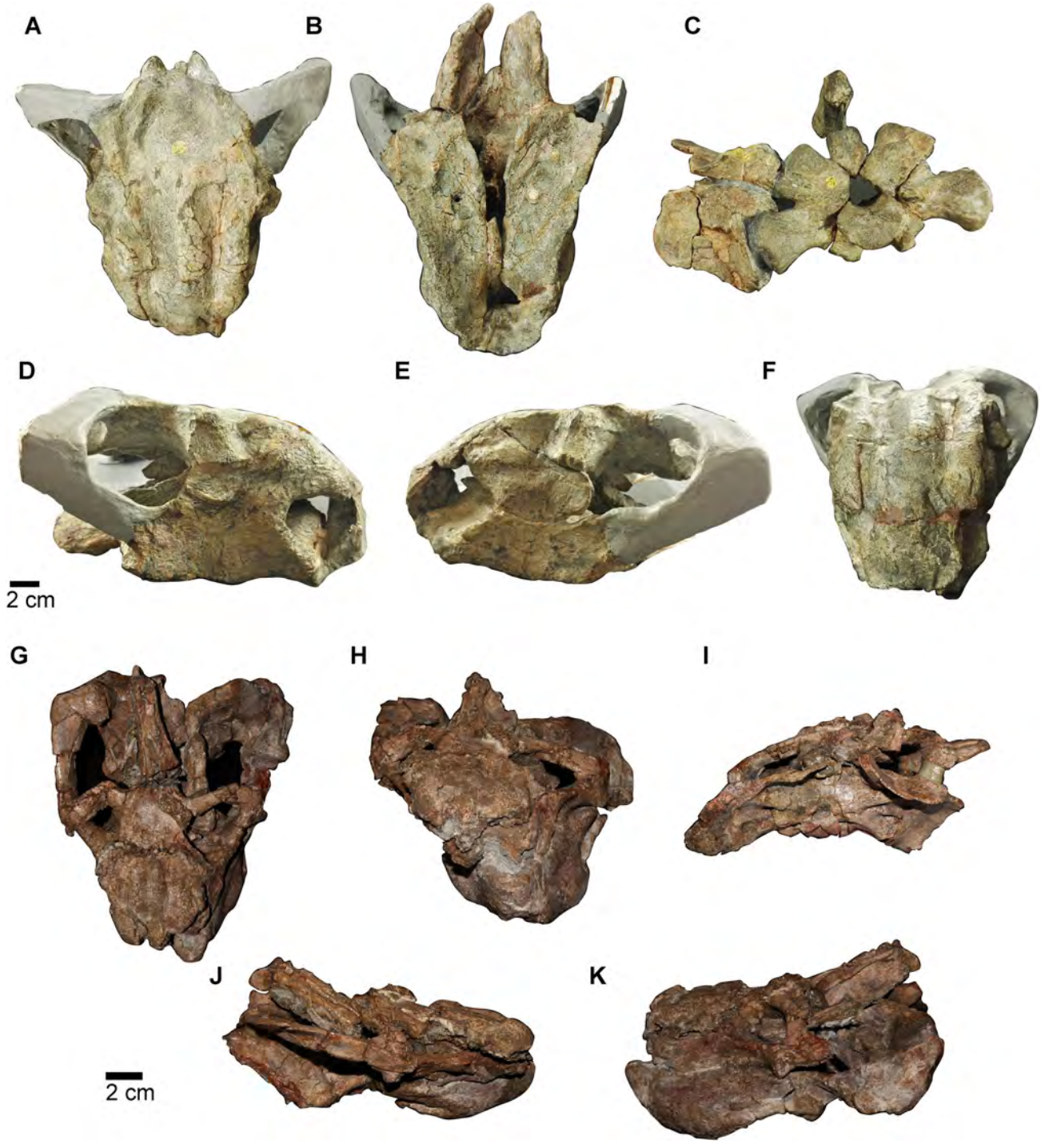

Figure 17. Comparison of skulls in clade B of the phylogenetic analysis, comparing specimens of '*Endothiodon uniseries*' and *E. tolani*. NHMUK PV R4044, *Endothiodon* cf. *bathystoma* ('*E. uniseries*') in **A**, dorsal, **B**, ventral, **C**, posterior, **D**, right lateral, **E**, left lateral and **F**, anterior views. NHCC LB 648, *Endothiodon* cf. *bathystoma* in **G**, dorsal, **H**, anterior, **I**, posterior, **J**, right lateral, and **K**, left lateral views.

Referred specimens. NMT RB162, NMT RB475, PPN2014-7, PPN2014-11, PPN2014-15, PPN2014-45, PPN2014-56, PPN2014-55, NHCC LB 780, NHCC LB 326, NMT RB162, NMT RB475.

Emended diagnosis. *Endothiodon* species with the following autapomorphies: presence of enlarged caniniforms; single tooth row; an oval pineal foramen surrounded by a thin collar of bone; and swollen prefrontals.

Endothiodon sp.

(Figs 10I, J, 11A, 12A–C)

Referred specimens. ISIR 203, ISIR 212, ISIR 218, ISIR 344, ISIR 341, ISIR 362, PPN2014-15, PPN2014-18, PPN2014-37, PPN2014-40, PPN2014-64, PPN2014-67, PPN2014-70, PPN2014-70-13B, ANHM FARB 5573, AMNH FARB 5613, AMNH FARB 5334, SAM-PK-3420, SAM-PK-581, CGP-T2, CGP/1/783, BP/1/1293, BP/1/3574, NHMUK PV R8173.

Justification. We classify specimens as *Endothiodon* sp. when there are preserved characters that allow determination as *Endothiodon* and at least one phylogenetic character is codable, but none of these characters is diagnostic of a specific species (e.g. pineal boss is diagnostic of *E. bathystoma*). For example, ISIR 344 has a notched premaxilla and ISIR 362 has grooves on the posterior surface of the opisthotic which are common to all three *Endothiodon* species, but absent in *Abajudon*.

Endothiodontia indet.

(Figs 8C–E, 9B–D, 10C, L, 11S, 12D–I)

Referred specimens. ISIR 207, ISIR 219, ISIR 345, ISIR 352, ISIR 354, ISIR 355, ISIR 361/1, ISIR 361/2, ISIR 363, ISIR 364, UEM 61, NHCC LB 11, NHCC LB 12, NHMUK PV R 1967, NHMUK PV R 7866, NHMUK R 12457, NHMUK R 12454; NHMUK R 12455; NHMUK R 36709; NHMUK R 36707, NHMUK R 12450, NHMUK R 12448, NHMUK R 12456, SAM-PK-10642, SAM-PK-1682, SAM-PK-3442, SAM-PK-628, SAM-PK-5605, SAM-PK-K6727, SAM-PK-7876, AM 3874, CGP uncatalogued, CGP/1/762, CGP/1/700, BP/1/4844, BP/1/5496, BP/1/7279, BP/1/7349, BP/1/7376.

Justification. Specimens which may have a broad morphological affinity with *Endothiodon* but have no codable characters. In this category, many partial mandibles with a single tooth row in which the tooth crowns are broken off are classified as Endothiodontia indet. because it is not possible to ascertain whether these specimens could be classified as *Abajudon*.

Dicynodontia indet.

(Fig. 10K)

Referred specimens. ISIR 359, ISIR uncatalogued, SAM-PK-3442.

Justification. SAM-PK-3442 and ISIR uncatalogued are undiagnosable osseous fragments. ISIR 359 is a fragment of the jugal, postorbital and maxilla.

Discussion

The validity of *E. mahalanobisi*

The phylogenetic analysis in this study identifies *E. mahalanobisi* as a distinct clade with a high Bremer support of 0.997 (Fig. 14B). This clade is morphologically and phylogenetically distinct from *E. tolani* specimens due to the absence of enlarged caniniforms, the lack of a collar of bone around the pineal foramen, and unswollen prefrontals. Key features of *E. mahalanobisi* include a narrow pineal foramen with no pineal boss or collar of bone, absence of enlarged caniniforms, shallow snout crests and flat prefrontals.

Interestingly, this species might have existed in Zambia and Mozambique, as well as India, according to similarities noted by Kammerer and Ordoñez (2021). NHCC LB 780 from Zambia, lacking enlarged caniniforms and bearing a resemblance to Indian *E. mahalanobisi*, may align more with this species than with the known *E. tolani* specimens from East Africa. The pineal foramen, like that in *E. mahalanobisi* ISIR 202, is on a flat surface. Despite overpreparation of NHCC LB 780, it remains morphologically similar to Indian *E. mahalanobisi*, with absence of enlarged caniniforms, a smooth dorsal snout, a triangular snout shape, a shallow ventral premaxillary excavation, a single maxillary tooth row and unswollen prefrontals. Its phylogenetic position in an experimental phylogenetic analysis where a collar of bone around the pineal foramen was coded as present remained unchanged (Supplemental material), suggesting NHCC LB 780 can be identified as *E. mahalanobisi*.

Previously, the presence of a single longitudinal medial snout ridge was considered an autapomorphy of *E. mahalanobisi* (Ray, 2000). However, due to the

difficulty in accurately defining and counting snout ridges in specimens with severe lateral compression, this study replaces 'snout ridges' with 'snout crest height'. Low snout crests are observed in *E. mahalanobisi* specimens but this trait is not exclusive to this species (Macungo et al., 2019; Maharaj et al., 2021).

Regarding sexual dimorphism, it is unlikely that the Zambian *E. mahalanobisi* specimens (e.g. NHCC LB 780) are a tuskless variant of *E. tolani*. If Indian *E. mahalanobisi* specimens are tuskless *E. tolani* individuals, some tusked specimens would have been found in the iron-rich nodules from the Kundaram Formation in in India, yet none are known (Bandyopadhyay & Ray, 2020), despite the majority of specimens being *Endothiodon* sp. Therefore, there is no evidence to consider Indian *E. mahalanobisi* a sexually dimorphic form of African *E. tolani*. On the other hand, the morphological similarities between Indian *E. mahalanobisi* specimens, Zambian NHCC LB 780, and Mozambican PPN2012-10-C3-1ß mentioned above suggest that these specimens may all belong to *E. mahalanobisi*, indicating a possible distribution of this species in India and East Africa.

The validity of *E. tolani*

NMT RB162, NHMUK PV R12443 and NMT RB475 are grouped into a clade identified as *E. tolani*. The unifying features for this clade, according to the analysis, include the presence of enlarged caniniforms, an oval pineal foramen encircled by a thin collar of bone, and swollen prefrontals, which serve as diagnostic traits for *E. tolani*. NHMUK PV R12443 and NMT RB475 share similar morphological traits, except for a larger tusk in NMT RB475, marking the first occurrence of such a robust tusk in *E. tolani* specimens, albeit broken at the front. For this analysis, enlarged caniniforms were considered only as a distinct trait due to the character's essential taxonomic significance in *E. tolani*. Should future discoveries yield more tusked specimens that reveal a wider range in tusk length and cross-section, incorporating this variation into the analysis will be crucial to better understand the phylogenetic positioning of *E. tolani*.

The validity of *E. bathystoma*

The phylogenetic analysis recognizes *E. bathystoma* as a distinct species (Fig. 14B and Table 5) based on diagnostic traits such as a circular pineal foramen on a robust pineal boss, absence of enlarged caniniforms, and swollen prefrontals. Specimens with robust pineal bosses present clear morphological differences in the skull roof compared to those lacking them. Absence of pineal bosses in '*E. uniseries*' specimens could be due to preservation bias, as these structures are fragile (Macungo et al., 2019). Among swollen prefrontals, NHMUK PV OR49414, CGP/1/709 and NHMUK PV R4042 show particularly robust swelling, likely indicating a more derived feature of *Endothiodon*.

NHMUK PV R4044 and NHCC LB 648 are tentatively reassigned to *Endothiodon* cf. *bathystoma*. These specimens are more complex as they show *E. tolani* and *E. bathystoma* traits. Namely, NHCC LB 648 has tusks, visible only in computed tomography data (K. Angielczyk, pers. comm., 2023). On the other hand, the prominent snout crests seen in *E. bathystoma* specimens support NHMUK PV R4044 and NHCC LB 648 as belonging to this species. The variable conditions of tusk presence in NHCC LB 648 and NHMUK PV R4044 at the base of the *E. bathystoma* clade might indicate either that in the Tanzanian *E. bathystoma* population this trait was potentially polymorphic, or that NHCC LB 648 was a transitional *E. bathystoma* specimen still retaining tusks. The fact that NHCC LB 648 possesses tusks brings the possibility that the presence of enlarged caniniforms in *E. tolani* is not sexually dimorphic. If enlarged caniniforms were sexually dimorphic in *E. bathystoma* there should be South African specimens with enlarged caniniforms, and none have ever been found. The phylogenetic analysis shows that the absence of enlarged caniniforms is a strong character that unites South African *E. bathystoma* specimens (with the exception of the Tanzanian specimen NHCC LB 648). It is, therefore, unlikely that enlarged caniniforms are a sexually dimorphic feature in *E. bathystoma* and *E. tolani*.

Similarly, determining sexual dimorphism by the presence of the pineal boss in *Endothiodon*, as for *Diictodon* (Sullivan et al., 2003), is challenging. Protruding pineal bosses are prone to breaking off at the base both during the post-mortem/preburial period and during exhumation, and as such the bone surface around the pineal foramen must be analysed carefully to look for any signs of breakage. South African Karoo specimens exhibit large *E. bathystoma*-like pineal bosses or lack skull preservation in that region. The absence of South African specimens that never developed a pineal boss suggests that this is not a sexually dimorphic character. However, more well-preserved *E. bathystoma* skulls could clarify this (Supplemental material; see also Angielczyk et al., 2014; Cox & Angielczyk, 2015; Macungo et al., 2019).

The phylogenetic analysis shows that tooth row count does not differentiate between the old *E. uniseries* species concept and the new *E. bathystoma* species concept, making it a taxonomic feature that needs to be used

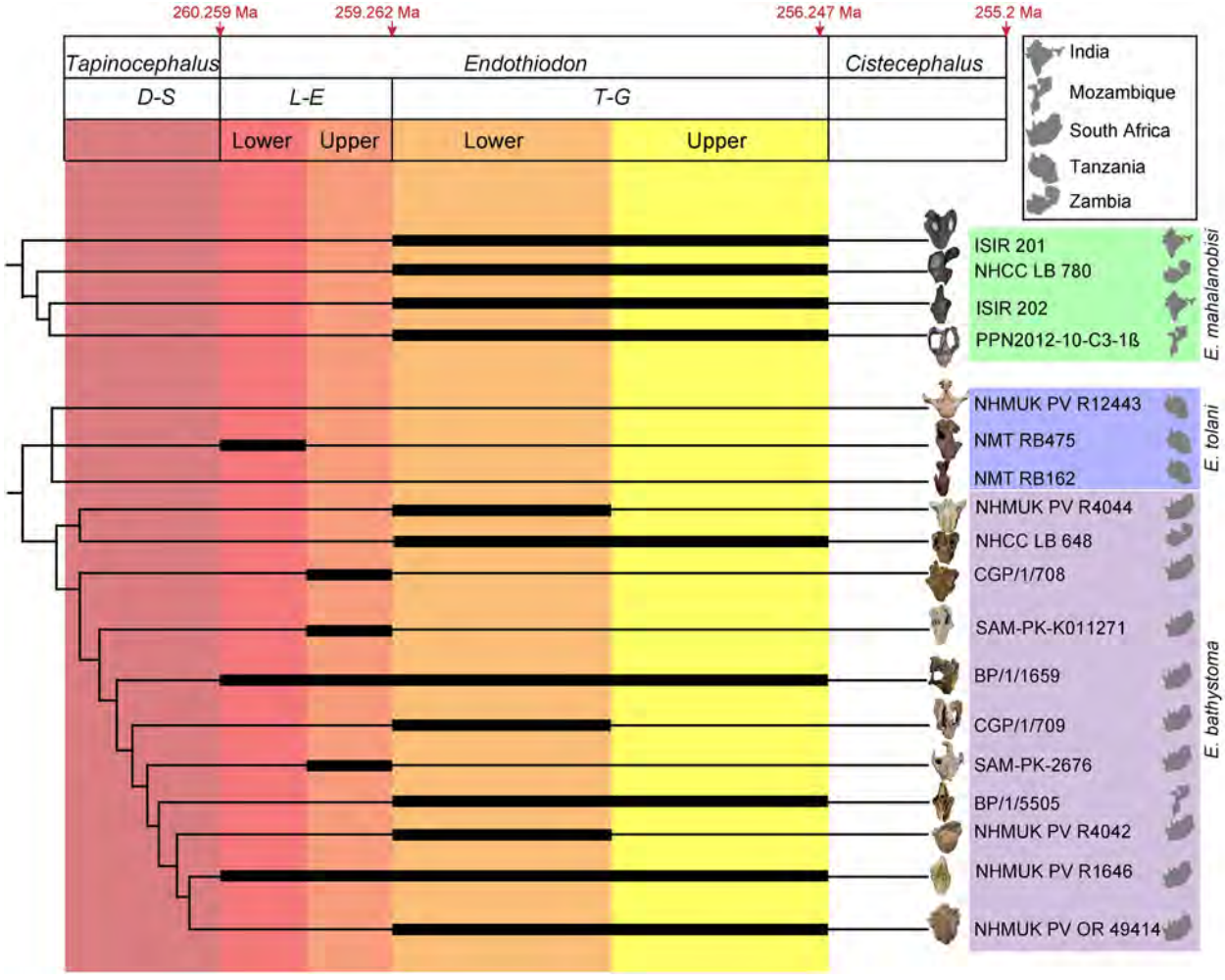

Figure 18. Phylogenetic tree mapped onto a stratigraphic column of the Karoo Basin Assemblage Zones and Subzones (based on Smith et al., 2020).

with caution. Importantly, we previously demonstrated that *Endothiodon* specimens of all size ranges can have single or multiple tooth rows, based on a sample of 38 *Endothiodon* mandibles from Mozambique (Macungo et al., 2019). However, by integrating information from the phylogenetic analyses and previous histological analyses of *Endothiodon* specimens (Olroyd et al., 2021), it is important to note that only *Endothiodon bathystoma* specimens have mandibular multiple tooth rows, namely NHMUK PV R1646 (the holotype of *E. bathystoma*), SAM-PK-K011271 and CGP/1/709. Whereas a specimen without multiple mandibular tooth rows may still be an *Endothiodon bathystoma* as other characters may be codable in the phylogenetic matrix (e.g. CGP/1/708, BP/1/5505), all specimens included in the phylogenetic matrix with mandible and skull preserved and mandibular multiple tooth rows were retrieved within the *E. bathystoma* species concept. Thus, isolated mandibles with multiple tooth rows can only be *E. bathystoma* (e.g. ISIR 206 and ISIR 202 from India; PPN2014-70-2 and UEM 01 from Mozambique; NHMUK PV R1696 and SAM-PK-K11131 from South Africa; NHCC LB 11 from Zambia; SAM-PK-10638 from Tanzania; and PV 0226P from Brazil). Similarly, but more rarely, specimens with maxillary multiple tooth rows should be regarded as *Endothiodon bathystoma* (i.e. SAM-PK-10642, SAM-PK-10639, NMT RB23), as can be exemplified by specimen AMNH FARB 5571. Regardless, these results imply that *E. uniseries* is here confidently subsumed within *E. bathystoma* due to the latter's nomenclatural priority under the regulations of the International Code of Zoological Nomenclature. Curiously, some previously identified *E. uniseries* specimens have multiple tooth rows (e.g. ISIR 204, NHMUK PV R4043). Additionally, previous classification of Indian specimens as *E. uniseries* (Ray, 2000), based on

Table 6. Approximate stratigraphic context of the three-species concept (*Endothiodon mahalanobisi*, *E. tolani*, *E. bathystoma*) in the phylogenetic analysis (based on the published literature and R. Smith, pers. comm.). Broken border indicates the possibility of NHCC LB 780 coming from the transition between subzones. **Abbreviations**: **D–S**, *Diictodon-Styracephalus* Subzone; **L–E**, *Lycosuchus-Eunotosaurus* Subzone.

Karoo Assemblage Zone	Karoo Subzone	Karoo Basin	K5c formation of Metangula Graben	Ruhuhu Formation	Luangwa Basin Upper Madumabisa Mudstone	Madumabisa Mudstone Formation of Mid Zambezi Basin	Kundaram Formation
Cistecephalus			*E. bathystoma*: NHCC LB11 *Endothiodon* sp. BP/1/3574				
Endothiodon (General Assemblage Zone) *E. bathystoma*: NHMUK PV R1646	*Tropidostoma-Gorgonops*	(General Subzone) *E. bathystoma*: NHMUK PV OR 49414 (Lower Subzone) *Endothiodon* cf. *bathystoma*: NHMUK-PV-R4044 *E. bathystoma*: NHMUK-PV- R4042 CGP/1/709	*E. mahalanobisi*: PPN2012-10- C3-1ß *E. bathystoma*: BP/ 1/5505				(General Subzone) *E. mahalanobisi*: ISIR 201 ISIR 202
	Lycosuchus-Eunotosaurus	(Upper Subzone) *E. bathystoma*: SAM-PK- K011271 CGP/1/708 SAM-PK-2676		(General Subzone) *E. tolani*: NMT RB162 NHMUK PV R12443 (Lower Subzone) *E. tolani*: NMT RB475		*E. mahalanobisi*: NHCC LB 780 *E. tolani* NHCC LB 648	
Tapinocephalus	*Diictodon-Styracephalus*						

size and robustness, is not supported here. Such characteristics are not deemed taxonomically valid. Hence, Indian *E. uniseries* may simply be larger *E. mahalanobisi* individuals, as shown by the phylogenetic analysis.

Biostratigraphic implications of the three-species concept

The calibrated phylogenetic analysis (Fig. 18) supports a three-species concept for *Endothiodon*: *E. mahalanobisi*, *E. tolani* and *E. bathystoma*. This concept is built on the tentative stratigraphic correlation of the *Endothiodon* specimens incorporated in the analysis (see Table 6). The findings raise important questions about *Endothiodon* speciation in southern/eastern Africa and India. Notably, the coexistence of *E. bathystoma*, *E. tolani* and *E. mahalanobisi* in the Metangula Graben of Mozambique is intriguing (Macungo et al., 2019). This is supported by the correlation of the Kundaram Formation in India, where *E. mahalanobisi* was originally found, with the *Tropidostoma-Gorgonops* Subzone of the Karoo Basin, where *E. bathystoma* has been discovered. Furthermore, in the late Permian, East African localities were palaeogeographically located in between the palaeo-oriental Indian localities and the palaeo-occidental South African localities (see the Supplemental material). There is also evidence suggesting the presence of both *E. bathystoma* and *E. tolani* in Tanzania. This is based on two large isolated pineal bosses from the upper Ruhuhu Formation (NHMUK PV R36708 and R36709, see the Supplemental material) assigned to *Endothiodon*, exhibiting the *E. bathystoma* morphotype (Angielczyk et al., 2014; Cox & Angielczyk, 2015). Similar findings have been observed in Mozambique (Macungo et al., 2019). With our analysis, along with the one conducted by Cox and Angielczyk (2015), it is now less unclear whether tusked *Endothiodon* represent the derived or basal condition. If enlarged caniniforms are the derived condition, *E. bathystoma* may have remained tuskless. This suggestion is supported by the findings of the current study, considering the basal placement of the tuskless *E. mahalanobisi* and the derived position of *E. bathystoma.* Analogously, the development of a large pineal boss in *E. bathystoma* is the apomorphic condition. Interestingly, however, the tusked Tanzanian specimen (NHCC LB 648) is placed basally in the *E. bathystoma* clade.

Cox and Angielczyk (2015) questioned whether Tanzanian *E. tolani* and *E. bathystoma* existed concurrently or in different periods. Their co-occurrence in Tanzania is supported by their geographical proximity; however, the strata in this part of the rift valley fill is heavily block-faulted and also lacks recognizable marker beds or datable tuffs. However, the *Endothiodon* record in the geographically close Mozambican Metangula Graben attests that co-existence of various *Endothiodon* species was possible. The Tanzanian specimens analysed here come from a biostratigraphic assemblage that correlates with South Africa's *Lycosuchus-Eunotosaurus* Subzone, where *E. bathystoma* is known (Day & Smith, 2020; K. Angielczyk, pers. comm., 2021).

On the other hand, the Luangwa basin specimens (BP/1/3574, NHCC LB11, NHCC LB12: Angielczyk et al., 2014) seem to disrupt the South African pattern where *Endothiodon* is restricted solely to the *Endothiodon* AZ. Importantly, the presence of multiple maxillary tooth rows in NHCC LB11 is diagnostic of *E. bathystoma*, hence making it the most recent occurrence of the species assuming that age is correctly estimated. Palynological and other dicynodont fossil data provides evidence that the endothiodontid specimens from the Luangwa Basin are from the *Cistecephalus*-equivalent AZ (Barbolini et al., 2016; Kammerer et al., 2021). Other *Endothiodon* Zambian specimens from the Mid-Zambezi Basin have recently been reassessed by Sidor et al. (2023) based on biostratigraphic information and attributed to the *Tropidostoma-Gorgonops* sub-AZ equivalent strata (e.g. NHCC LB 236, NHCC LB 322, NHCC LB 628; which were not analysed in the course of this study). The two specimens analysed here from the Mid-Zambezi Basin are NHCC LB 780 (here classified as *E. mahalanobisi*) and NHCC LB 648 (here classified as *Endothiodon* cf. *bathystoma*); they were not included in Sidor et al. (2023). NHCC LB 780 comes from a locality with a faunal assemblage consistent with *Endothiodon* AZ taxa (K. Angielczyk pers. comm., 2024). However, the NHCC LB 648 locality also preserved a dinocephalian taxon, potentially placing it in the *Tapinocephalus* AZ, but except for this dinocephalian fossil the faunal assemblage is consistent with the *Endothiodon* AZ, which raises the question whether the dinocephalian fossil has been transported post-mortem (K. Angielczyk, pers. comm., 2024).

Deposits in India and Brazil containing *Endothiodon* correlate with South Africa's *Endothiodon* AZ (Boos et al., 2013; Day & Smith, 2020; Holz et al., 2010). These locations also feature tuskless *Endothiodon* specimens, potentially indicating the persistence of tuskless *Endothiodon* after the end-Guadalupian mass extinction. The Brazilian *Endothiodon* specimens were found with tapinocephalid fossils (Boos et al., 2015), suggesting it could be older. However, this correlation is broadly stratigraphic, making their exact ages uncertain (Boos et al., 2015). Nevertheless, we confirm the presence of *E. bathystoma* in Brazil due to the presence of multiple tooth rows and a pineal boss on PV0226P. In sum, our taxonomic review confirms *Endothiodon bathystoma* in

all austral basins from Brazil and South Africa in the palaeo-west, to India in the palaeo-east of Pangaea, including in the Chiweta Beds in Malawi where Haughton (1926) described a specimen with multiple tooth rows.

Conclusions

This is the first study to determine the relationships of the specimens within the genus *Endothiodon* using phylogenetic analyses, in conjunction with their stratigraphic positions. The hypothesis was that there are three taxonomically valid *Endothiodon* species: *E. tolani*, *E. bathystoma* and *E. mahalanobisi*, following Cox and Angielczyk (2015). The phylogenetic and anatomical distinctions of these three species in this study do not refute this hypothesis. *Endothiodon mahalanobisi* is retrieved as a distinct species diagnosed by the absence of enlarged caniniforms, the presence of a slit-like or narrow pineal foramen (which differs from the collared pineal foramen of *E. tolani* and the large pineal boss of *E. bathystoma*), and unswollen or flat prefrontals, which are swollen in all other *Endothiodon* species. Furthermore, our study suggests the exclusive presence of *E. mahalanobisi* in India but we demonstrate its presence in East Africa for the first time. The analysis also supports the synonymy of '*E. uniseries*' with *E. bathystoma*. Only 18 *Endothiodon* skulls were used in this analysis, however, because the rest were too fragmentary (Supplemental material), so future phylogenetic analyses will depend on additional *Endothiodon* discoveries. In other *Endothiodon*-bearing deposits outside the Karoo Basin, this study suggests that a more *E. bathystoma*-like morphotype (i.e. a large pineal boss and the loss of enlarged caniniforms) may be a more derived condition of *Endothiodon* skull morphology. Further biostratigraphic refinement, especially in other Gondwanan deposits outside the Karoo Basin, will allow for a more detailed undertaking of similar analyses in the future, which would result in clearer insights into the relationship between *Endothiodon* morphological evolution and their depositional environments.

Acknowledgements

We thank Kenneth Angielczyk for access to photographs of Tanzanian and Zambian *Endothiodon* specimens and for helpful advice about *Endothiodon* research, and also Christian Kammerer for photographs of American Museum of Natural History specimens of *Endothiodon*. Michael Day granted access to specimens housed at the Natural History Museum (London, UK) and is thanked for feedback and helpful discussions on the biostratigraphy of *Endothiodon* in South Africa. Saswati Bandyopadhyay is thanked for access to specimens at the Indian Statistical Institute (Kolkata, India).

We are grateful to the following South African collection curators and managers for access to South African *Endothiodon* specimens: Zaituna Skosan, Claire Browning and the Karoo Palaeontology team (Iziko South African Museum, Cape Town); Julien Benoit, Bernhard Zipfel and Sifelani Jirah (Evolutionary Studies Institute, University of Witwatersrand, Johannesburg); Nonhlanhla Mchunu (Council for Geosciences, Pretoria); and Rose Prevec (Albany Museum, Grahamstown). Mark Young is also thanked for helping on the Systematic palaeontology section. We thank the reviewers (Kenneth D. Angielczyk and Michael Day) for their reviews which greatly improved the original version of the manuscript.

This research formed part of IEMM's PhD, which was supported by an Innovation Doctoral Scholarship and an Extended Support Scholarship from the National Research Foundation of South Africa (grant numbers 112375 and 130780, respectively) as well as support from the Palaeontological Scientific Trust (PAST), Johannesburg, South Africa. RA and ZM were funded by FCT – AGA KHAN Development Network (grant number 333206718). RS and AC were funded by NRF/African Origins Platform (grant numbers 82607 and 136510, respectively). ZM was also funded by Palaeontological Scientific Trust (PAST). Accession to the fossils in the Museu Nacional de Geologia is also gratefully acknowledged.

Supplemental material

Supplemental material for this article can be accessed here: https://doi.org/10.1080/14772019.2024.2346578

Disclosure statement

No potential conflict of interest was reported by the author(s).

References

Angielczyk, K. D. (2001). Preliminary phylogenetic analysis and stratigraphic congruence of the dicynodont anomodonts (Synapsida: Therapsida). *Palaeontologia Africana*, *37*, 53–79.

Angielczyk, K. D. (2007). New specimens of the Tanzanian dicynodont '*Cryptocynodon*' *parringtoni* Von Huene, 1942

(Therapsida, Anomodontia), with an expanded analysis of Permian dicynodont phylogeny. *Journal of Vertebrate Paleontology*, *27*(1), 116–131. https://doi.org/10.1671/0272-4634(2007)27[116:NSOTTD]2.0.CO;2

Angielczyk, K. D., **Benoit, J.**, & **Rubidge, B. S.** (2021). A new tusked cistecephalid dicynodont (Therapsida, Anomodontia) from the Upper Permian Upper Madumabisa Mudstone Formation, Luangwa Basin, Zambia. *Papers in Palaeontology*, *7*(1), 405–446. https://doi.org/10.1002/spp2.1285

Angielczyk, K. D., & **Kammerer, C. F.** (2017). The cranial morphology, phylogenetic position, and biogeography of the upper Permian dicynodont *Compsodon helmoedi* van Hoepen (Therapsida, Anomodontia). *Papers in Palaeontology*, *3*(4), 513–545. https://doi.org/10.1002/spp2.1087

Angielczyk, K. D., **Steyer, J. S.**, **Sidor, C. A.**, **Smith, R. M.**, **Whatley, R. L.**, & **Tolan, S.** (2014). Permian and Triassic dicynodont (Therapsida: Anomodontia) faunas of the Luangwa Basin, Zambia: Taxonomic update and implications for dicynodont biogeography and biostratigraphy. In C. F. Kammerer, K. D. Angielczyk, & J. Fröbisch (Eds.), *Early evolutionary history of the Synapsida* (pp. 93–138). Springer.

Araújo, R., **Fernandez, V.**, **Rabbitt, R. D.**, **Ekdale, E. G.**, **Antunes, M. T.**, **Castanhinha, R.**, **Fröbisch, J.**, & **Martins, R. M. S.** (2018). Endothiodon cf. bathystoma (Synapsida: Dicynodontia) bony labyrinth anatomy, variation and body mass estimates. *PLoS One*, *13*(3), e0189883. https://doi.org/10.1371/journal.pone.0189883

Araújo, R., **Smith, R. M. H.**, **Tolan, S.**, **Angielczyk, K. D.**, **Crowley, J.**, **Milisse, D.**, & **Mugabe, J.** (2020). Biostratigraphic refinement of tetrapod-bearing beds from the Metangula Graben (Niassa Province, Mozambique): New radiometric dating and the first Lower Triassic tetrapod fossils from Mozambique. *Palaeontologia Africana*, *54*, 56–68.

Bandyopadhyay, S., & **Ray, S.** (2020). Gondwana vertebrate faunas of India: Their diversity and intercontinental relationships. *Episodes*, *43*(1), 438–460. https://doi.org/10.18814/epiiugs/2020/020028

Barberena, M. C., & **Araújo, D. C.** (1975). Tetrápodos fósiles de Sudamérica y deriva continental. *Actas 1° Congreso Argentino de Paleontología y Bioestratigrafia*, *1*, 497–504.

Barberena, M. C., **Araújo, D. C.**, & **Lavina, E. L.** (1985). Late Permian and Triassic tetrapods of southern Brazil. *National Geographic Research/Winter*, *1985*, 5–20.

Barbolini, N., **Bamford, M. K.**, & **Tolan, S.** (2016). Permo–Triassic palynology and palaeobotany of Zambia: A review. *Palaeontologia Africana*, *50*, 18–30.

Boos, A. D. S., **Kammerer, C. F.**, **Schultz, C. L.**, & **Neto, V. P.** (2015). A tapinocephalid dinocephalian (Synapsida, Therapsida) from the Rio do Rasto Formation (Paraná Basin, Brazil): taxonomic, ontogenetic and biostratigraphic considerations. *Journal of South American Earth Sciences*, *63*, 375–384. https://doi.org/10.1016/j.jsames.2015.09.003

Boos, A. D. S., **Schultz, C. L.**, **Vega, C. S.**, & **Aumond, J. J.** (2013). On the presence of the Late Permian dicynodont *Endothiodon* in Brazil. *Palaeontology*, *56*(4), 837–848. https://doi.org/10.1111/pala.12020

Broili, F., & **Schröder, J.** (1936). Beobachtungen an Wirbeltieren der Karroo-formation. 16. *Beobachtungen am Schädel von* Emydochampsa *Broom*. Sitzungsberichte der mathematischnaturwissenschaftlichen Abteilung der Bayerischen Akademie der Wissenschaften zu München, *1936*, 21–44.

Broom, R. (1900). On the structure of the palate in *Dicynodon*, and its allies. *Transactions of the South African Philosophical Society*, *11*(1), 169–176. https://doi.org/10.1080/21560382.1900.9525963

Broom, R. (1904a). On some points in the anatomy of the anomodont skull. *Records of the Albany Museum*, *1*(2), 69–88.

Broom, R. (1904b). On the structure and affinities of the endothiodont reptiles. *Transactions of the South African Philosophical Society*, *15*(1), 259–282. https://doi.org/10.1080/21560382.1904.9626441

Broom, R. (1904c). On two new endothiodont genera (*Prodicynodon* and *Opisthoctenodon*). *Records of the Albany Museum*, *1*, 69–73.

Broom, R. (1904d). Notice of a new endothiodont genus (Chelyoposaurus). *Records of the Albany Museum*, *1*, 184.

Broom, R. (1911). On some new south African Permian reptiles. *Proceedings of the Zoological Society of London*, *81*, 1073–82. https://doi.org/10.1111/j.1096-3642.1911.tb01976.x

Broom, R. (1912). On some new fossil reptiles from the Permian and Triassic beds of South Africa. *Proceedings of the Zoological Society of London*, *82*, 859–876. https://doi.org/10.1111/j.1469-7998.1912.tb07564.x

Broom, R. (1913). A revision of the reptiles of the Karroo. *Annals of the South African Museum*, *7*, 361–366.

Broom, R. (1915). Catalogue of types and figured specimens of fossil vertebrates in the American Museum of Natural History. II. – Permian, Triassic and Jurassic reptiles of South Africa. *Bulletin of the American Museum of Natural History*, *25*, 105–164.

Broom, R. (1921). On some new genera and species of anomodont reptiles from the Karroo beds of South Africa. *Proceedings of the Zoological Society of London*, *91*, 647–674. Wiley Online Library. https://doi.org/10.1111/j.1096-3642.1921.tb03286.x

Broom, R. (1923). On the structure of the skull in the carnivorous dinocephalian reptiles. *Proceedings of the Zoological Society of London*, *82*, 661–684. https://doi.org/10.1111/j.1096-3642.1923.tb02203.x

Broom, R. (1932). *The mammal-like reptiles of South Africa and the origin of mammals*. Witherby.

Castanhinha, R., **Araújo, R.**, **Júnior, L. C.**, **Angielczyk, K. D.**, **Martins, G. G.**, **Martins, R. M. S.**, **Chaouiya, C.**, **Beckmann, F.**, & **Wilde, F.** (2013). Bringing dicynodonts back to life: Paleobiology and anatomy of a new emydopoid genus from the Upper Permian of Mozambique. *PLoS ONE*, *8*(12), e80974. https://doi.org/10.1371/journal.pone.0080974

Cluver, M. A., & **King, G. M.** (1983). A reassessment of the relationships of Permian Dicynodontia (Reptilia, Therapsida) and a new classification of dicynodonts. *Annals of the South African Museum*, *91*(3), 195–273.

Cox, C. B. (1964). On the palate, dentition, and classification of the fossil reptile Endothiodon and related genera. *American Museum Novitates*, No. 2171. Retrieved from http://digitallibrary.amnh.org/handle/2246/3347

Cox, C. B., & **Angielczyk, K. D.** (2015). A new endothiodont dicynodont (Therapsida, Anomodontia) from the Permian Ruhuhu Formation (Songea Group) of Tanzania and its

feeding system. *Journal of Vertebrate Paleontology*, *35*(4), e935388. https://doi.org/10.1080/02724634.2014.935388

Day, M. O., & **Rubidge, B. S.** (2020). Biostratigraphy of the *Tapinocephalus* Assemblage Zone (Beaufort Group, Karoo Supergroup), South Africa. *South African Journal of Geology*, *123*(2), 149–164. https://doi.org/10.25131/sajg.123.0012

Day, M. O., & **Smith, R. M. H.** (2020). Biostratigraphy of the *Endothiodon* Assemblage Zone (Beaufort Group, Karoo Supergroup), South Africa. *South African Journal of Geology*, *123*(2), 165–180. https://doi.org/10.25131/sajg.123.0011

Dias-da-Silva, S. (2012). Middle–Late Permian tetrapods from the Rio Do Rasto Formation, Southern Brazil: A biostratigraphic reassessment. *Lethaia*, *45*(1), 109–120. https://doi.org/10.1111/j.1502-3931.2011.00263.x

Fröbisch, J. (2009). Composition and similarity of global anomodont-bearing tetrapod faunas. *Earth-Science Reviews*, *95*(3–4), 119–157. https://doi.org/10.1016/j.earscirev.2009.04.001

Goloboff, P. A., & **Catalano, S. A.** (2016). TNT Version 1.5, including a full implementation of phylogenetic morphometrics. *Cladistics*, *32*(3), 221–238. https://doi.org/10.1111/cla.12160

Goloboff, P. A., **Farris, J. S.**, & **Nixon, K. C.** (2008). TNT, a free program for phylogenetic analysis. *Cladistics*, *24*(5), 774–786. https://doi.org/10.1111/j.1096-0031.2008.00217.x

Haughton, S. H. (1926). On Karroo vertebrates from Nyasaland. *South African Journal of Geology*, *29*(1), 69–83.

Holz, M., **França, A. B.**, **Souza, P. A.**, **Iannuzzi, R.**, & **Rohn, R.** (2010). A stratigraphic chart of the Late Carboniferous/Permian succession of the eastern border of the Paraná Basin, Brazil, South America. *Journal of South American Earth Sciences*, *29*(2), 381–399. https://doi.org/10.1016/j.jsames.2009.04.004

Jacobs, L. L., **Winkler, D. A.**, **Newman, K. D.**, **Gomani, E. M.**, & **Deino, A.** (2005). Therapsids from the Permian Chiweta beds and the age of the Karoo Supergroup in Malawi. *Palaeontologia Electronica*, *8*, 28A.

Kammerer, C. F., **Araújo, R.**, **Cumbane, K.**, **Macungo, Z.**, **Smith, R. M.**, & **Angielczyk, K. D.** (2021). New material of *Dicynodon angielczyki* (Synapsida: Anomodontia) from Mozambique and Zambia with biostratigraphic implications for African Permo–Triassic basins. *Journal of Vertebrate Paleontology*, *41*(6), e2041652. https://doi.org/10.1080/02724634.2021.2041652

Kammerer, C. F., & **Ordoñez, M.**, **de los A.** (2021). Dicynodonts (Therapsida: Anomodontia) of South America. *Journal of South American Earth Sciences*, *108*(June), 103171. https://doi.org/10.1016/j.jsames.2021.103171

Keyser, A. W. (1993). A re-evaluation of the smaller Endothiodontidae. *Memoir of the Geological Survey of South Africa*, *82*, 1–53.

Kitching, W. (1963). The fossil localities and mammal-like reptiles of the upper Luangwa Valley, Northern Rhodesia. *South African Journal of Science*, *7*.

Latimer, E. M., **Gow, C. E.**, & **Rubidge, B. S.** (1995). Dentition and feeding niche of *Endothiodon* (Synapsida; Anomodontia). *Palaeontologia Africana*, *32*, 75–82.

Lydekker, R. (1890). Family Endothiodontidae. *Catalogue of Fossil Reptilia and Amphibia*, *4*, 64–66.

Macungo, Z., **Araújo, R.**, **Browning, C.**, **Smith, R. M. H.**, **David, R.**, **Angielczyk, K. D.**, **Massingue, A.**, **Ferreira-Cardoso, S.**, & **Kortje, D. J. P.** (2023). Novel anatomy and paleobiological insights on Cistecephalus microrhinus (Synapsida: Dicynodontia). In Y.-N. Lee (Ed.), *Windows into sauropsid and synapsid evolution* (pp. 1–65). Dinosaur Science Center Press.

Macungo, Z., **Loide, I.**, **Zunguza, S.**, **Nhamutole, N.**, **Maharaj, I. E. M.**, **Mugabe, J.**, **Angielczyk, K. D.**, & **Araújo, R.** (2019). *Endothiodon* (Therapsida, Anomodontia) specimens from the Middle/Late Permian of the Metangula Graben (Niassa Province, Mozambique) increase complexity to the taxonomy of the genus. *Journal of African Earth Sciences*, *163*, 103647. https://doi.org/10.1016/j.jafrearsci.2019.103647

Maddison, W. P. (2008). Mesquite: A modular system for evolutionary analysis. *Evolution*, *62*, 1103–1118.

Maddison, W. P., & **Maddison, D. R.** (2021). Mesquite: A modular system for evolutionary analysis. (Version 3.70). Retrieved from http://www.mesquiteproject.org

Maharaj, I. E. M., **Chinsamy, A.**, & **Smith, R. M. H.** (2021). The postcranial anatomy of *Endothiodon bathystoma* (Anomodontia, Therapsida). *Historical Biology*, *33*(7), 1066–1088. https://doi.org/10.1080/08912963.2019.1679128

Matthews, S. C. (1973). Notes on open nomenclature and on synonymy lists. *Palaeontology*, *16*(4), 713–719.

Olroyd, S. L., **LeBlanc, A. R. H.**, **Araújo, R.**, **Angielczyk, K. D.**, **Duhamel, A.**, **Benoit, J.**, & **Amaral, M.** (2021). Histology and μCT reveal the unique evolution and development of multiple tooth rows in the synapsid *Endothiodon*. *Scientific Reports*, *11*(1), 16875. https://doi.org/10.1038/s41598-021-95993-6

Olroyd, S. L., **Sidor, C. A.**, & **Angielczyk, K. D.** (2017). New materials of the enigmatic dicynodont *Abajudon kaayai* (Therapsida, Anomodontia) from the Lower Madumabisa Mudstone Formation, Middle Permian of Zambia. *Journal of Vertebrate Paleontology*, *37*(6), e1403442. https://doi.org/10.1080/02724634.2017.1403442

Owen, R. (1859). On some reptilian remains from South Africa. *Edinburgh New Philosophical Journal*, *10*, 289–291.

Owen, R. (1860). On the orders of fossil and recent Reptilia, and their distribution in time. *Report of the Twenty-Ninth Meeting of the British Association for the Advancement of Science*, *1859*, 153–166.

Owen, R. (1876). *Descriptive and illustrated catalogue of the fossil Reptilia of South Africa in the collection of the British museum* (pp. xii + 88, 70 pls). Taylor and Francis.

Owen, R. (1879). On the endothiodont Reptilia, with evidence of the species Endothiodon uniseries, Ow. *Quarterly Journal of the Geological Society*, *35*(1–4), 557–564. https://doi.org/10.1144/GSL.JGS.1879.035.01-04.38

Ray, S. (2000). Endothiodont dicynodonts from the Late Permian Kundaram Formation, India. *Palaeontology*, *43*(2), 375–405. https://doi.org/10.1111/1475-4983.00132

Ray, S., & **Bandyopadhyay, S.** (2003). Late Permian vertebrate community of the Pranhita–Godavari Valley, India. *Journal of Asian Earth Sciences*, *21*(6), 643–654. https://doi.org/10.1016/S1367-9120(02)00050-0

Rubidge, B. S., **Erwin, D. H.**, **Ramezani, J.**, **Bowring, S. A.**, & **De Klerk, W. J.** (2013). High-precision temporal calibration of Late Permian vertebrate biostratigraphy: U-Pb zircon constraints from the Karoo Supergroup, South

Africa. *Geology*, *41*(3), 363–366. https://doi.org/10.1130/G33622.1

Seeley, H. G. (1892). On further evidence of *Endothiodon bathystoma* (Owen) from Oude Kloof in the Nieuwveldt Mountains, Cape Colony. *Quarterly Journal of the Geological Society*, *48*(1–4), 476–480. https://doi.org/10.1144/GSL.JGS.1892.048.01-04.32

Seeley, H. G. (1894). Researches on the structure, organisation and classification of the fossil Reptilia. Part 9. Sect. 1. On the Therosuchia. *Philosophical Transactions of the Royal Society of London. Series B, Containing Papers of a Biological Character*, *185*, 987–1018.

Sidor, C. A., **Mann, A.**, & **Angielczyk, K. D.** (2023). *Gorgonops* and *Endothiodon* (Synapsida: Therapsida) from the Madumabisa Mudstone Formation: Evidence of a previously unreported tetrapod biozone in the Mid-Zambezi Basin of southern Zambia. *Journal of Vertebrate Paleontology*, *43*(1), e2256812. https://doi.org/10.1080/02724634.2023.2256812

Smith, R. M. H. (2020). Biostratigraphy of the Cistecephalus Assemblage Zone (Beaufort Group, Karoo Supergroup), South Africa. *South African Journal of Geology*, *123*(2), 181–190. https://doi.org/10.25131/sajg.123.0013

Smith, R. M. H., **Rubidge, B. S.**, **Day, M. O.**, & **Botha, J.** (2020). Introduction to the tetrapod biozonation of the Karoo Supergroup. *South African Journal of Geology*, *123*(2), 131–140. https://doi.org/10.25131/sajg.123.0009

Sullivan, C., & **Reisz, R. R.** (2005). Cranial anatomy and taxonomy of the late Permian dicynodont *Diictodon*. *Annals of the Carnegie Museum*, *74*(1), 45–75. https://doi.org/10.2992/0097-4463(2005)74[45:CAATOT]2.0.CO;2

Sullivan, C., **Reisz, R. R.**, & **Smith, R. M.** (2003). The Permian mammal-like herbivore Diictodon, the oldest known example of sexually dimorphic armament. *Proceedings. Biological Sciences*, *270*(1511), 173–178. https://doi.org/10.1098/rspb.2002.2189

Toerien, M. J. (1953). The evolution of the palate in South African Anomodontia and its classificatory significance. *Palaeontologia Africana*, *1*, 49–117.

van Hoepen, E. C. N. (1934). Oor die indeling van die Dicynodontidae na aanleiding van nuwe vorme. *Palaeontologiese Navorsing van die Nasionale Museum, Bloemfontein*, *2*, 67–101.

Whitney, M. R., **Angielczyk, K. D.**, **Peecook, B. R.**, & **Sidor, C. A.** (2021). The evolution of the synapsid tusk: Insights from dicynodont therapsid tusk histology. *Proceedings of the Royal Society B*, *288*(1961), 20211670. https://doi.org/10.1098/rspb.2021.1670

Associate Editor: Richard Butler